Atmos. Meas. Tech. Discuss., https://doi.org/10.5194/amt-2019-104
Manuscript under review for journal Atmos. Meas. Tech.
Discussion started: 18 April 2019

Atmospheric Measurement Techniques Discussions

Inter-comparison of the Elemental and Organic Carbon Mass Measurements from Three North American National Long-term Monitoring Networks

Tak W. Chan[1,*], Lin Huang[1,*], Kulbir Banwait[2], Wendy Zhang[1], Darrell Ernst[1], Xiaoliang Wang[3], John G. Watson[3], Judith C. Chow[3], Mark Green[3], Claudia I. Czimczik[4], Guaciara M. Santos[4], Sangeeta Sharma[1], Keith Jones[5]

[1] Climate Chemistry Measurements and Research, Climate Research Division, Environment and Climate Change Canada, 4905 Dufferin Street, Toronto, Ontario, Canada, M3H 5T4

[2] Measurements and Analysis Research Section, Air Quality Research Division, Environment and Climate Change Canada, 4905 Dufferin Street, Toronto, Ontario, Canada, M3H 5T4

[3] Division of Atmospheric Sciences, Environmental Analysis Facility, Desert Research Institute, 2215 Raggio Parkway, Reno, NV 89512

[4] Earth System Science, University of California, Irvine, CA 92697-3100, USA

[5] Applied Environmental Prediction Science Pacific & Yukon, Prediction Services Operations West, Prediction Services Directorate, Meteorological Service of Canada, #201-401 Burrard Street, Vancouver, B.C., Canada, V6C 3S5

* Corresponding authors, Email: tak.chan@canada.ca, Phone: (416) 739-4419; lin.huang@canada.ca, Phone: (416) 739-5821

Keywords

Black carbon, thermal evolution, air pollution, carbonaceous aerosol, IMPROVE, CAPMoN, CABM

Atmos. Meas. Tech. Discuss., https://doi.org/10.5194/amt-2019-104
Manuscript under review for journal Atmos. Meas. Tech.
Discussion started: 18 April 2019

Atmospheric Measurement Techniques Discussions

Abstract

Carbonaceous aerosol is a major contributor to the total aerosol load and being monitored by diverse measurement approaches. Here, ten years of continuous carbonaceous aerosol measurements collected at the Centre of Atmospheric Research Experiments (CARE) in Egbert, Ontario, Canada on quartz filters by three independent networks (Interagency Monitoring of PROtected Visual Environments (IMPROVE), Canadian Air and Precipitation Monitoring Network (CAPMoN), and Canadian Aerosol Baseline Measurement (CABM)) were compared. Specifically, the study evaluated how differences in sample collection and analysis affected the yield of total carbon (TC), organic carbon (OC), and elemental carbon (EC). When all measurements were normalized with respect to concentration measured in a common reference year, OC measurements agreed to within 29-48% and EC measurement to within 20% amongst the different networks. Fitted with a sigmoid function, elevated OC and EC concentrations were found when ambient temperature exceeded 10 °C. These increased ambient concentrations of OC during summer were attributed to the secondary organic aerosol (SOA) formation and forest fire emissions, while elevated EC concentrations were attributed to forest fire emissions and increased vehicle emissions. The observations from this study suggest that carbonaceous aerosol measurements, especially EC, can be synchronized across networks if sample collection and analytical method in each network remain internally consistent. This study allows the generation of regional to continental-scale-harmonized concentration data sets for benchmarking of atmospheric chemical transport models that determine emission sources and sinks, and assess the effectiveness of government mitigation policies in improving air quality and reducing reliance on fossil fuel consumption.

Introduction

Carbonaceous aerosols, including organic carbon (OC) and elemental carbon (EC; often referred to as black carbon (BC)), make up a large fraction of the atmospheric particulate matter (PM) mass. Atmospheric OC and EC particles that are emitted directly into the atmosphere have both natural (e.g., biomass burning or forest fires) and anthropogenic (e.g., internal combustion engines) sources. A significant amount of the particulate OC is also formed in the atmosphere through oxidation and condensation of volatile organic compounds (e.g., isoprene and terpenes), which are emitted directly from vegetation. BC is a by-product of incomplete combustion of hydrocarbon fuels, generated mainly from fossil fuel combustion and biomass burning. Atmospheric particles have direct and indirect influences on climate, visibility, air quality, ecosystems, and adverse human health effects (Bond et al., 2013; Japar et al 1986; Lesins et al., 2002; Watson, 2002). Atmospheric BC absorbs solar radiation while

OC scatters (Schulz et al., 2006). However, BC and OC co-exist in atmospheric particles and the net radiative forcing of the aerosol particles depends on the particle size, composition, and the mixing state of the particles, while all of these variables also change as aerosol particles age (Fuller et al., 1999; Lesins et al., 2002). Long-term atmospheric OC and EC measurements provide necessary benchmark data for understanding inter-annual trends and seasonal variations and for constraining BC sources (Collaud Coen et al. 2013). They are also needed for determining changes of emissions and their impacts on atmospheric processing and developing/verifying the effectiveness of future environmental and health-related policies (Chen et al. 2012).

Conducting long-term ambient BC mass measurements is challenging in part due to the lack of a universally accepted definition of BC. The scientific community generally accepts the definitions from Bond et al. (2013) that BC particles possess the following properties: (1) strongly absorbing in the visual spectrum with an inverse wavelength (λ) dependence (i.e., λ^{-1}) (Bond and Bergstrom 2006), (2) refractory in nature with a vaporization temperature near 4000 K (Schwarz et al., 2006), (3) insoluble in water and common organic solvents (Fung 1990), (4) aggregate form (Kittelson, 1998), and (5) chemically inertness in the atmosphere, as graphitic carbon (Bond et al. 2013). BC is a generic term in the literature and is often interchanged with other terms such as EC, soot, refractory BC, light absorbing carbon, or equivalent BC (Petzold et al 2013). The use of different terminology is linked to the different methodologies used to measure different physical or chemical properties of BC. In this study, the term BC is referred to a substance that absorbs a significant amount of visible light and was created during incomplete combustion, from either internal combustion engines or biomass burning. EC is referred to the carbon mass determined from the thermal evolution analysis (TEA) or thermal optical analysis (TOA) of carbonaceous materials at the highest temperature set point (e.g., >550 °C) under an oxygenated environment. It is also assumed that ambient EC and BC concentrations resemble each other.

TOA and TEA have been applied in many long-term monitoring networks with various protocols to quantify OC and EC concentrations from aerosol deposits on quartz-fiber filters (Birch and Cary, 1996; Cachier et al., 1989; Cavalli et al., 2010; Chow et al., 1993; Huang et al., 2006; Huntzicker et al., 1982) due to the simplicity in filter sample collection and the analytical procedures. TOA and TEA provide a direct measurement of carbon mass as part of the gravimetric PM mass. One of the limitations of TOA and TEA is the need for sufficient sampling time to accumulate enough mass for precise measurements (i.e., ensuring a high signal to noise ratio) which constrains the temporal resolution of such samples. In addition, EC and OC are defined differently in different protocols and could affect the absolute mass

84 values measured. Generally, OC is quantified under a pure helium (He) atmosphere at a low heating
85 temperature whereas EC is quantified under an oxygen (O_2)/He atmosphere at high temperatures.
86 Estimates of total carbon (TC=OC+EC) derived from TOA and TEA methods are generally consistent,
87 whereby OC estimates agree within 10-20%, but larger differences are found for EC, owing to its smaller
88 contribution to TC (Cavalli et al., 2010; Chow et al., 1993; 2001; 2005; Countess 1990; Watson et al.,
89 2005).

90 During thermal analysis, some of the OC chars to form pyrolyzed organic carbon (POC) when
91 heated in the inert He atmosphere, darkening the filter (Chow et al., 2004; Watson et al. 2005). When
92 O_2 is added, POC combusts with EC and leads to an overestimation of EC in the PM deposit. The
93 formation of POC depends on the nature of the organic materials, the amount of the oxygenated
94 compounds in the collected particles, the rate, duration, and temperature of the heating, and the supply
95 of O_2 in the carrier gas (Cachier et al. 1989; Chan et al., 2010; Han et al. 2007; Yang and Yu, 2002). POC
96 in TOA is estimated by monitoring reflectance and/or transmittance of a 633-650 nm laser beam, with
97 the resulting EC method termed thermal optical reflectance (TOR) or thermal optical transmittance
98 (TOT). When the reflected or transmitted laser signal returns to its initial intensity at the start of the
99 analysis (i.e., at OC/EC split point), it is assumed that artifact POC has left the sample and the remaining
100 carbon belongs to EC. The carbon mass before the split point is defined as OC whereas that after the
101 split point is defined as EC. POC is defined as the mass determined between the time when O_2 is
102 introduced and the OC/EC split point.

103 Quartz-fiber filters adsorb organic vapors (Chow et al., 2009; Turpin et al., 1994; Viana et al.,
104 2006; Watson et al., 2010), resulting in non-PM contributions to OC and charring enhancement within
105 the filter. These vapors are adsorbed passively when the filter is exposed to air and more so as air is
106 drawn through the filter during PM sampling. Sampling at low filter face velocities for long period of
107 time could lead to more adsorption (McDow and Huntzicker, 1990), while using high filter face velocities
108 for longer sample durations may result in evaporation of semi-volatile compounds as negative artifact
109 (Khalek, 2008; Sutter et al., 2010; Yang et al., 2011). The positive OC artifact from adsorption usually
110 exceeds the negative evaporation artifact, especially at low temperatures, resulting in OC
111 overestimation. This can be corrected by subtracting the OC concentration from field blanks or backup
112 filters located downstream of a Teflon-membrane or quartz-fiber filter (Chow et al., 2010; Watson et al.,
113 2005; 2010).

Previous studies further suggested that TOT could over-estimate the POC mass more than TOR, resulting in higher POC (and lower EC) because of the charring of the adsorbed organic vapors within the filter (Chow et al 2004; Countess 1990). Since only a portion (0.5-1.5 cm^2) of the filter is analyzed, inhomogeneous PM deposits add to measurement uncertainty when OC and EC are normalized to the entire filter deposit area. Deposits that are light or too dark can cause unstable laser signals that affect the OC/EC split (Watson et al., 2005).

This study evaluated the consistency and comparability of co-located carbonaceous aerosol measurements by three North American networks (IMPROVE, CAPMoN, CABM) over 10 years. These networks use different sampling instruments, frequencies, and durations, analytical methods, and artifact corrections. The investigation identified potential issues and determined solutions for improving the compatibility of the different measurements. When combining all measurements from all networks at various sites, it offers the possibility to create a regional- to continental-scale, harmonized carbon concentration dataset, which is important and necessary for constraining model input for understanding the OC and EC sources.

Sampling and Measurements

Sampling Site

The sampling station is the Center for Atmospheric Research Experiments (CARE) located near Egbert, Ontario (44°12′ N, 79°48′ W, 251 m a.s.l.), Canada. This station is owned and operated by Environment and Climate Change Canada (ECCC), and is located 70 km NNW of the city of Toronto. There are no major local anthropogenic sources within about 10 km of the site. Air that reaches this site from southern Ontario and the northeastern United States typically carries urban or anthropogenic combustion pollutants that were emitted within last two days (Rupakheti et al. 2005; Chan and Mozurkewich 2007; Chan et al., 2010). Air from the north generally contains biogenic emissions and is often accompanied with the presence of SOA during summer (Chan et al., 2010; Slowik et al., 2010). Table 1 compares the instrument and analytical specifications among the three networks.

The IMPROVE Network

The IMPROVE network, established in 1987, includes regional-scale monitors for detecting visibility trends, understanding long-range transport, and evaluating atmospheric processes (Malm 1989; Yu et al. 2004). IMPROVE operates about 150 sites and provides long-term records of PM_{10} and

143 $PM_{2.5}$ (particles with aerodynamic diameter less than 10 and 2.5 microns, respectively) mass as well as
144 $PM_{2.5}$ composition, including anions (i.e., chloride, nitrate, and sulfate), and carbon (OC and EC).
145 IMPROVE 24-hour samples at Egbert were acquired once every third day from 2006 to 2015. The
146 sampling period was from 0800 to 0800 local standard time (LST) except for August 16, 2006 through
147 October 24, 2008 (from 0000 to 0000 LST). Module C of the IMPROVE sampler uses a modified air-
148 industrial hygiene laboratory (AIHL) cyclone with a 2.5 µm cut point at a flow rate of 22.8 liters per
149 minute (L/min). PM samples were collected onto a 25 mm diameter quartz-fiber filter (Tissue quartz,
150 Pall Life Sciences, Ann Arbor, MI, USA), which were pre-fired at 900°C for four hours. Once sampled,
151 filters were stored in freezer until they were ready to be analyzed. All samples were analyzed by the
152 IMPROVE_A thermal/optical reflectance protocol (Figure S1a; Supplementary information) (Chow et al.,
153 2007) as shown in Table S1 (Supplementary information). The IMPROVE measurements (denoted as
154 IMPROVE_A TOR) were obtained from the website http://vista.cira.colostate.edu/IMPROVE (Malm et
155 al., 1994; IMPROVE, 2017).

156 ***The CAPMoN Network***

157 CAPMoN was established in 1983 to understand the source impacts of acid rain-related
158 pollutants from long-range transport to the Canadian atmosphere and soil. The network operates 30
159 regionally representatives sites (as of 2015) across Canada with most located in Ontario and Quebec.
160 Measurements include PM, trace gases, mercury (both in air and precipitation), tropospheric ozone, and
161 multiple inorganic ions in air and precipitation (https://www.canada.ca/en/environment-climate-
162 change/services/air-pollution/monitoring-networks-data/canadian-air-precipitation.html).

163 Twenty-four-hour samples (0800 to 0800 LST) were acquired every third day from 2005 to 2015
164 using the Modified Rupprecht and Patashnick (R&P) Model 2300 $PM_{2.5}$ Speciation Sampler with
165 ChemComb cartridges and $PM_{2.5}$ impactor plates with impactor foam to direct particles onto a 47 mm
166 diameter tissue quartz-fiber filter operated at 10 L/min (Thermo Scientific, Waltham, MA, USA). A
167 second parallel cartridge is configured with a 47 mm front Teflon-membrane filter and a quartz-fiber
168 backup filter to estimate vapor adsorption artifact. All quartz-fiber filters were pre-fired at either 800°C
169 or 900°C for over two hours and cooled at 105°C overnight and stored in freezer (-15 °C) before being
170 used for sampling. All sampled filters were also stored in freezer until they are ready for analysis.

171 Carbon was determined using the Sunset laboratory-based carbon analyzer
172 (http://www.sunlab.com/) following the IMPROVE-TOT protocol from 2005 to 2007 (denoted as Sunset-

TOT), then by DRI Model 2001 Thermal/Optical Carbon Analyzer following the IMPROVE-TOR protocol (denoted as DRI-TOR) from 2008 to 2015 (Chow et al., 1993). As shown in Table S1, the temperature settings for IMPROVE (i.e., DRI-TOR) protocol for CAPMoN samples are lower than those of IMPROVE_A protocol for IMPROVE samples by 20°C to 40°C (Figure S1b). This small difference in the temperature-ramp between these protocols results in correlated but different OC, EC, and TC mass (Chow et al., 2007).

The ECCC Canadian Aerosol Baseline Network

The Climate Chemistry Measurements and Research (CCMR) Section in the Climate Research Division of ECCC has operated the Canadian Aerosol Baseline Measurement (CABM) network since 2005 to acquire data relevant to climate change (https://www.canada.ca/en/environment-climate-change/services/climate-change/science-research-data/greenhouse-gases-aerosols-monitoring/canadian-aerosol-baseline-measurement-program.html). The CABM network includes 6 sites (as of 2016) for aerosol chemical, physical, and optical measurements that cover ecosystems at costal, interior urban/rural areas, boreal forests, and the Arctic. Measurements are intended to elucidate influences from various emission sources on regional background air, including biogenic emissions, biomass burning as well as anthropogenic contributions from industrial/urban areas.

The CABM filter pack system uses a $PM_{2.5}$ stainless steel cyclone (URG-2000-30EHS) operated at 16.7 L/min for sampling from 2006 to 2015 with an operator manually changing the 47 mm quartz-fiber filter on a weekly basis. All quartz-fiber filters were pre-fired at 900°C overnight prior being sampled. Once sampled, filters were stored in freezer until they were ready to be analyzed. A TEA method, EnCan-Total-900 (ECT9), developed by Huang et al. (2006) and refined later (Chan et al., 2010), was used to analyze the OC, POC, and EC on the quartz-fiber filters using a Sunset laboratory-based carbon analyzer. The ECT9 protocol was developed to permit stable carbon isotope (^{13}C) analysis of the OC and EC masses without causing isotope fractionation, as it was demonstrated by Huang et al. (2006). This method first heats the filter at 550°C and 870°C for 600 s each in the He atmosphere to determine OC and POC (including carbonate carbon; CC), respectively, and then combusts the sample at 900°C under 2% O_2 and 98% He atmosphere for 420 s to determine EC (Figure S1c and Table S1). The ECT9 POC definition (released as CO_2 at 870 °C) includes the charred OC, and some calcium carbonate ($CaCO_3$) that decomposes at 830°C, as well as any refractory OC that is not combusted at 550°C. Chan et al. (2010) found that POC determined by ECT9 was proportional to the oxygenated compounds (e.g., aged aerosol from atmospheric photochemical reaction) and possibly humic-like materials. Consistent with the

IMPROVE_A TOR protocol (Chow et al., 2007), OC is defined as the sum of OC and POC, as CC is usually negligible in $PM_{2.5}$.

CABM sites are also equipped with Particle Soot Absorption Photometer (PSAP; Radiance Research, Seattle, WA, USA) that monitor aerosol light absorption as changes in the amount of light transmitted through a quartz-fiber filter. Assuming the mass absorption coefficient (MAC) for aerosol is constant at Egbert, the one minute PSAP absorption measurements is linearly proportional to the BC or EC oncentrations.

Differences in Sampling and Analysis among Networks

Depending on the sharpness (i.e., slope) of the inlet sampling effectiveness curve (Watson et al., 1983), different size-selective inlets may introduce measurement uncertainties. CAPMoN uses an impactor whereas CABM and IMPROVE use cyclones. Impactor may have larger pressure drops across the inlet that might enhance semi-volatile PM evaporation. Larger solid particles might bounce when in contact with the impactor and be re-entrained in the $PM_{2.5}$ samples if the impactor is overloaded (Flagan and Seinfeld, 1998; Hinds, 1999). Atmospheric mass size distributions typically peak at about 10 µm with a minimum near 2.5 µm, therefore, the difference in mass collected with different impactors or cyclones among the three networks is not expected to be large (Watson and Chow, 2011).

The small filter disc (25 mm diameter) and high flow rate (22.8 L/min) in the IMPROVE sampler result in a 5- to 7-fold higher filter face velocity (i.e., 107.7 versus 16-20 cm/s) than that for the CAPMoN and CABM samplers. McDow and Huntzicker (1990) assert that higher filter face velocity may reduce sampling artifacts. However, very high face velocity (>100 cm/s) may enhance OC volatilization (Khalek 2008).

Both CAPMoN and IMPROVE networks correct for vapor adsorption, while CABM network does not. CAPMoN subtracts the organic artifact from the parallel channel, whereas IMPROVE (up until 2015) used monthly median OC values obtained from the backup quartz-filters from 13 sites (not including Egbert).

Multiple studies show that using the same TOA protocol on both DRI and Sunset carbon analyzers can produce comparable TC concentrations. However, large differences in EC are found between the reflectance and transmittance POC correction (Chow et al., 2004; 2005; Watson et al., 2005). Difference in OC and EC definitions among different TOA and TEA protocols introduce

233 measurement uncertainties. Among the TOA methods, how POC is determined from the laser signals at
234 different temperatures in the inert He atmosphere introduce uncertainties. Large uncertainties in laser
235 transmittance were found for lightly- and heavily-loaded samples (Birch and Cary, 1996). For the CABM
236 samples, the POC determined at 870 °C by ECT9 represents different OC properties and does not equal
237 the charred OC obtained by Sunset-TOT, DRI-TOR, or IMPROVE_A TOR.

238 **NIST urban dust standard comparison (SRM 8785 & 1649a)**

239 The consistency of the OCEC measurements obtained between the ECT9 and the IMPROVE_A
240 method was assessed by measuring four replicates of the National Institute of Standards and
241 Technology (NIST) Urban Dust Standard Reference Material (SRM) 8785 (Cavanagh and Watters, 2005;
242 Klouda et al., 2005). These samples were produced by resuspension of the original SRM 1649a urban
243 dust sample, followed by collection of the fine fraction ($PM_{2.5}$) on quartz-fiber filters (Klouda et al., 2005;
244 May and Trahey, 2001). Past studies on SRM 1649a and SRM 8785 have shown consistent composition
245 (Currie et al., 2002; Klouda et al., 2005). The SRM 8785 filters with mass loading of 624-2262 μg were
246 analyzed following the ECT9 method by the ECCC laboratory and the IMPROVE_A protocol by the DRI
247 laboratory during 2009-2010.

248 Figure 1 shows reasonable correlations with 21-25% higher TC and EC by the ECT9 method. The
249 values in the SRM 8785 certificate were reported as grams of OC or EC per grams of PM mass, which are
250 average mass ratios based on analysis of a small numbers of randomly selected samples. Figure 2 shows
251 that IMPROVE_A protocol by DRI compared well with the certificate values. Ratios measured with ECT9
252 were greater, but not significantly different from the certificate values.

253 The parameter EC/TC, calculated based on the reported certificate values, were compared with
254 the average EC/TC values determined from the inter-comparison study (ICP) by the DRI group (using
255 IMPROVE_A) and the ECCC group (using ECT9) (Fig. 2d). These results show that EC/TC reported by both
256 DRI and CCMR were statistically the same as the certificate value.

257 Finally, the EC/TC value was further verified by analyzing multiple SRM 1649a sample with the
258 ECT9 method. The combusted CO_2 from OC, EC, and TC were analyzed for the isotope ratios (i.e.,
259 $^{14}C/^{12}C$) expressed as a fraction of modern carbon (i.e., FM_i is the ratio of $^{14}C/^{12}C$ in the sample i, relative
260 to a modern carbon standard) for individual mass fractions (i.e., FM_{TC}, FM_{OC}, and FM_{EC}). Using isotopic
261 mass balance, the EC/TC ratio can be derived from Eq. [1]:

$$FM_{TC} = FM_{OC} \times \left(1 - \frac{EC}{TC}\right) + FM_{EC} \times \frac{EC}{TC} \quad [1]$$

The $^{14}C/^{12}C$ abundances were determined by off-line combustion method at the Keck Carbon Cycle accelerator mass spectrometry (KCCAMS) Facility at University of California Irvine. A FM_{TC} value of 0.512 was obtained, which is close to certificate values that range from 0.505 to 0.61 (Currie et al., 2002). Average measured values of FM_{OC} and FM_{EC} for the SRM 1649a via ECT9 were 0.634 (n=3) and 0.349 (n=3), respectively. This yields an EC/TC ratio of 0.425, close to the reported certificate value of 0.49 and the IMPROVE_A value of 0.47 (Figure 2d), reconfirming a good separation of OC from EC using the ECT9 method.

Results and Discussion

Weekly versus 24-hour Samples

Comparing two years of Egbert measurements (2005-2007), Yang et al. (2011) suggested that integrated weekly samples may experience reduced vapor adsorption but increased losses of semi-volatile organics leading to lower OC measurements. Weekly EC values were higher than those from 24-hour samples, which were attributed to the higher analytical uncertainties for the lower loadings on the 24-hr samples (Yang et al., 2011). Here, the effect of different sample duration on EC concentrations is assessed using five years (2010-2015) of real-time (1 min average) PSAP particle light absorption measurements (at 567 nm). The results demonstrate that both data sets capture the variations adequately (Figure 3a) with correlated monthly averages (Figure 3b). Figure 3c shows a good correlation (r=0.78) between the weekly and every third day 24-hour samples with a slope of 0.96. Assuming the variations in light absorption can represent the variations in EC, these results suggest that monthly averaged EC based on weekly sampling is about 4% lower.

Vapor Adsorption Corrections

Figure 4 shows the carbon concentration time series with and without the artifact correction for CAPMoN samples. Vapor adsorption contributes to a large amount of the measured OC (Figure 4a), but a negligibly amount to EC (Figure 4b) and POC after 2008 (Figure 4c). The median vapor adsorption artifact was 0.79 µg/m^3 from 2008 to 2015 for DRI-TOR, representing about 50.9% of the uncorrected OC, compared to 0.92 µg/m^3 (43.3% of uncorrected OC) using the Sunset-TOT before 2008 (Supplemental Figure S2). Least square regressions between corrected and uncorrected carbon in Figure 5 shows a slope of 0.52 for OC and 0.56 for TC with good correlations (r=0.93-0.94). Sunset-TOT

291 measurements acquired prior 2008 are mostly scattered around the regression line, with higher
292 concentrations. On average, about 48% of the uncorrected OC (0.84 μg/m^3) can be attributed to vapor
293 adsorption. The low filter face velocity (15.5 cm/s) in CAPMoN samples could be one of the contributing
294 factors.

295 Figure 5c indicates that EC concentrations are 7.8% (0.02 μg/m^3) lower after artifact correction.
296 These levels are close to the detection limit of 0.022 μg/m^3 and within analytical uncertainties (Chow et
297 al., 1993). Some Sunset-TOT EC measurements are scattered from the regression line, indicating a more
298 accurate and consistent adsorption correction for DRI-TOR (Figure 5b). Although not expected to impact
299 EC concentration, vapor adsorption directly affects POC correction and thus influences EC mass
300 determination.

301 Figure 5d shows that 4.3% (0.01 μg/m^3) of POC was caused by vapor adsorption using the DRI-
302 TOR protocol. For Sunset-TOT (red open circles), however, up to 21.1% (0.17 μgC/m^3) of the POC was
303 detected on the backup filter. Filter transmittance is influenced by both surface and within filter
304 charring and EC from different sources have been observed to have different filter penetration depths
305 (Chen et al., 2004; Chow et al., 2004), an optical correction by reflectance appears to be more
306 appropriate when POC/EC ratio in measurements are high. Regardless, the absolute POC and EC
307 concentrations were much lower than OC and the adsorption correction on TC is mostly attributed to
308 the OC artifact.

309 Since the CAPMoN aerosol deposits were acquired at a low filter face velocity (15.5 cm/s), it is
310 expected that the magnitude of the vapor adsorption correction would be smaller for the IMPROVE
311 samples due to the use of higher filter face velocity. This is supported by the observations from Watson
312 et al. (2009) at six anchor IMPROVE sites, suggesting that vapor adsorption obtained from backup quartz
313 filters represented about 23% of the uncorrected OC values, whereas those obtained from field blanks
314 were averaged to be about 18%. In comparison with the IMPROVE measurements at Egbert, the vapor
315 adsorption obtained from field blank represent about 16% (or 0.18 μg/m^3) of the uncorrected OC
316 measurements. Filter fibers are saturated over a long sampling interval (Khalek, 2008; Watson et al.,
317 2009), thus, artifacts for the CABM samples are expected to be lower relatively.

318 **CAPMoN vs. IMPROVE Measurements**

319 Temporal variations of DRI-TOR CAPMoN measurements are comparable to the IMPROVE_A
320 TOR protocol (Figure 6), showing a similar temporal pattern with elevated peaks found in mid-summer

(July). High correlations are found for DRI-TOR OC and TC with IMPROVE_A measurements (r=0.90-0.91; Table 2) while lower correlations (r=0.78-0.79) are seen for Sunset-TOT data. Good correlations are observed between the DRI-TOR and IMPROVE_A TOR POC measurements (r=0.85) but much lower correlations are observed for Sunset-TOT and IMPROVE_A POC measurements (r=0.70). Correlations between DRI-TOR EC and IMPROVE_A TOR EC are high (r=0.81) but it is not the case between Sunset-TOT EC and IMPROVE_A TOR EC (r=0.33).

When fitting DRI-TOR and Sunset-TOT measurements to IMPROVE_A TOR measurements through the origin (i.e., Regression 1) typically yields less than unity slopes (0.64-0.97; Table 2), suggesting that the carbonaceous masses reported by CAPMoN were in general lower than IMPROVE. Fitting the measurements allowing an intercept (i.e., Regression 2) typically yields least square slopes close to unity (>0.92) with small intercepts.

The effect of using transmittance or reflectance for POC determination is apparent. The Sunset-TOT POC correction is larger because transmittance is affected by the charred OC within the filter. This is consistent with the larger regression slopes in POC (Regression 1: 1.8) between Sunset-TOT and IMPROVE_A TOR protocol than the slope in POC (1.0) between the DRI-TOR and IMPROVE_A TOR protocol.

CABM vs. IMPROVE Measurements

Figure 6 shows the temporal variations of the ECT9 CABM measurements with other networks. The temporal variations of the CABM measurements were consistent with the temporal trends of measurements from the other two networks. While ECT9 OC concentrations are comparable (±~15%) with the IMPROVE_A TOR measurements, higher TC and EC concentrations are found in CABM samples.

The ECT9 versus IMPROVE_A Regression 1 slopes are equal to or greater than unity, ranging from 1.2 to 1.8 (Table 2). Linear regression with intercept (i.e., Regression 2) yields lower slopes (0.6-1.7) with positive intercepts (0.06-0.18 $\mu g/m^3$), signifying higher TC and EC concentrations for ECT9 samples. Higher intercepts (0.12-0.18 $\mu g/m^3$) for TC, OC, and POC are consistent with ECT9 measurements uncorrected for vapor adsorption. The ECT9 method yielded 66-83% higher EC than IMPROVE_A TOR, with moderate correlation (r=0.74). Differences in combustion temperatures, OC/EC split, inhomogeneous deposition of mass loading on filter spots could contribute to these discrepancies. Heating under an oxidative environment at a constant temperature of 900 °C in the ECT9 protocol could

combust more highly refractory carbon than the IMPROVE_A protocol, which only heats progressively from 580 °C to 840 °C. When plotted on different scales, Figure S3 shows that the two EC data sets track well, capturing both long-term trends and short-term variations.

A slope approaching unity (1.00) was obtained when fitting the ECT9 POC to IMPROVE_A TOR POC through the origin (Figure 7d). Refitting the data allowing an intercept leads to a slope of 0.62 with a y-intercept (0.12; Table 2), comparable in magnitude to the vapor adsorption artifact. The correlation coefficient between ECT9 POC and IMPOVE_A TOR POC is low (r=0.46; Table 3). However, there is a significant correlation found between the IMPROVE_A TOR POC and IMPROVE_A TOR OC (r=0.91), and even to a lesser extent between IMPROVE_A TOR POC and IMPROVE_A TOR EC (r=0.71). In comparison, ECT9 POC has weak correlation with ECT9 OC (r=0.65) and ECT9 EC (r=0.37).

Comparison of the Normalized Time Series

Measurements from the networks are normalized in Figure 8 to assess the comparability as follows:

$$[x]'_t = [x]_t/[x]_{to} \qquad [2]$$

Where $[x]'_t$ is the normalized concentration at time t; $[x]_t$ and $[x]_{to}$ are monthly carbonaceous aerosol mass concentrations at time t and in January 2008, respectively. Figure 8 also includes the monthly average temperatures (green dotted curve), wind speed and direction (in the form of wind barb).

Normalized TC from the three networks correlate well (r≥0.79; Table 3). Figure 8a shows that normalized TC values tracked each other and represented the annual pattern, with DRI-TOR showing the largest TC, followed by IMPROVE_A TOR and ECT9. TC concentrations peaked around each July which experienced the highest temperatures.

Comparable temporal variations among these networks are also found for EC (Figure 8c) with good correlations (r=0.69-0.81). Figure 9e shows that DRI-TOR and IMPROVE_A TOR EC tracked well (slope of 1.03±0.02) with greater scatter for the ECT9 samples (slope=1.125) during summer (May-Oct in Figure 9f; defined based on ambient temperature).

Temporal variations of the normalized OC (Figure 8b) are similar to TC variations with high correlations (r=0.86-0.90; Table 3). However, large variations were found in Regression slopes from 0.71 to 1.32 (Table 4).

Figures 9c and 9d show that OC measurements were higher during summer (May-October). Monthly wind roses (Figures S4) show prevailing winds from the NW during summer. Air masses reaching Egbert during summer represent a mixture of the anthropogenic emissions from the south and the biogenic emissions from the north. Intense solar radiation received during summer could result in increased SOA formation. The limited solar radiation during winter hindered the SOA formation resulting in less data scatter. The extent of organic vapor desorption may be enhanced for the week-long samples in CABM network during summer.

The largest variations are found for POC (Figure 8d) with the lowest normalized POC concentrations found for ECT9 samples. Table 3 shows that POC concentrations are correlated with OC for both IMPROVE_A TOR and DRI-TOR samples (r=0.91-0.92) but not for ECT9 samples (r=0.65). POC from DRI-TOR and IMPROVE_A TOR samples also correlated (r=0.85), but not with ECT9 samples (r=0.44-0.46). These observations shows that the POC definition in ECT9 is not just a charred OC correction but likely include the characterization of other oxygenated organic materials (Chan et al., 2010). Additional research is needed to verify if the increased SOA formation during the summer season could increase the variation of the ECT9 POC with POC defined by other methods.

Seasonality in Carbon

A sigmoid function was applied to characterize the relationship between carbon and ambient temperature. The Sigmoid function has a characteristic "S" shape and represents an integral of a Gaussian function. Figure 9 shows elevated carbon during summer, consistent with the observations from Yang et al. (2011) and Healy et al. (2017). Relationships between carbon concentrations and ambient temperatures are shown in Figure S5. Apparent increases in OC and TC concentrations are found when ambient temperatures exceed about 10 °C; a phenomenon not as apparent in EC. EC from the week-long CABM samples are more scattered.

The TC, OC, and EC from all measurements are averaged and shown in Figure 10 with the following best-fitted sigmoid functions:

$$TC = 1.053 + \left\{\frac{3.558}{1+exp\left(\frac{23.081-T}{3.760}\right)}\right\} \quad [3]$$

$$OC = 0.780 + \left\{\frac{1.838}{1+exp\left(\frac{20.089-T}{2.978}\right)}\right\} \quad [4]$$

405 $$EC = 0.239 + \left\{\frac{1.446}{1+exp\left(\frac{34.776-T}{8.404}\right)}\right\} \quad [5]$$

406 Equations [3]-[5] show that lower limits of the observed TC, OC, and EC concentrations are 1.05, 0.78,
407 and 0.24 μgC/m^3, with the half way of the maximum growth curve occurring at about 23 °C, 20 °C, and
408 35 °C, respectively. The predicted maximum concentrations for TC, OC, and EC are 4.61, 2.62, and 1.69
409 μgC/m^3, respectively.

410 To determine the air mass origins, a Lagrangian particle dispersion transport model (FLEXible
411 PARTicle dispersion model; FLEXPART) (Stohl et al., 2005) was applied to obtain daily five-day back-
412 trajectories from Egbert from 2006 to 2015. Figure S6 summarizes the average FLEXPART footprints for
413 summer (May-Oct) and winter (Nov-Apr) seasons, showing the probability of air masses originating from
414 various regions. These results indicate regional contributions from boreal forest in the northern part of
415 Ontario and Quebec, as well as anthropogenic emissions from the northern U.S. Five-day trajectories
416 show larger concentrations from the N and NW, consistent with wind roses shown in Figure S4.

417 At low ambient temperatures, primary emissions (e.g., local transportation, residual heating,
418 and industrial activities) account for most of the ambient OC and EC (Ding et al., 2014). Increased
419 human activities (e.g., traveling by car and barbecuing) during warmer weather could lead to increased
420 emissions. High ambient temperature also leads to increased biogenic emissions (e.g., monoterpenes)
421 from the boreal forest and increased SOA formation (Chan et al., 2010; Leaitch et al., 2011; Passonen et
422 al., 2013; Tunved et al., 2006). The central and eastern boreal forest fire season typically occurs from
423 May to August when ambient air is dry and hot, resulting in generally increased OC and EC emissions
424 (Lavoué et al 2000). Transboundary transport of biomass burning emissions from the U.S. could also
425 contribute to the higher concentrations in southern Ontario (Healy et al. 2017). Increasing ambient
426 temperature from 10 °C to 20 °C leads to higher OC concentrations from 0.84 to 1.61 μgC/m^3 (91.7%
427 increase) and EC concentration from 0.31 to 0.45 μgC/m^3 (45.2% increase). The temperature
428 dependency of OC and EC suggests a potential climate feedback mechanism consistent with the
429 observations from Leaitch at al. (2011) and Passonen et al. (2013).

430 Chan et al. (2010) showed that ECT9 POC possesses a positive relationship with oxygenated
431 organics and aged aerosol particles. The seasonality in ECT9 POC is compared with the average OC and
432 EC seasonality observed at Egbert (Figure 10d). Interestingly, the ECT9 POC concentration does not
433 show a gradual exponential shape of function as for OC and EC (Figures 10b and 10c). Instead, it shows

434 a small but obvious two-step function when plotted against ambient temperature. The ECT9 POC results
435 (Figure 10d) suggest constant sources of background emissions of possible oxygenated organic
436 compounds with additional secondary formation at higher temperatures (e.g., >15 °C). Future study is
437 needed to verify this.

438 **Conclusions**

439 Ten years of OC and EC measurements at Egbert were obtained from three independent
440 networks (IMPROVE, CAPMoN, CABM). Differences in carbon concentrations were attributed to
441 different sampling methods, analytical protocols, and filter artifact corrections. Vapor adsorption did
442 not affect EC values but contributed about 48% (or 0.84 μg/m^3) of the measured OC for the CAPMoN
443 network with the lowest filter face velocity of 15.5 cm/s. When sampling at a filter face velocity of 108
444 cm/s, the IMPROVE field blanks account for about 16% (or 0.18 μg/m^3) of the measured OC. TC
445 measurements differences were influenced by the uncorrected vapor adsorption artifact as a result of
446 the OC artifact as in the CABM measurements. Pyrolyzed OC (POC) from both DRI-TOR (i.e., IMPROVE)
447 and IMPROVE_A TOR protocols correlated with OC (r=0.91-0.92), indicative of the charring property of
448 the measured OC. ECT9 POC was only weakly correlated with OC (r=0.65) and had weak correlations
449 with POC from DRI-TOR and IMPROVE_A TOR (r=0.44 and 0.46), suggesting ECT9 POC includes
450 compounds with different properties under high temperature gasification (870 °C).

451 Analyzing the SRM 8785 standard reference samples demonstrate the consistency in long-term
452 carbon measurements. Although the inter-comparison of SRM 8785 samples showed 20-25% higher TC
453 and EC by ECT9 method, no statistical difference was found for the EC/TC ratios, which was further
454 supported by isotope measurements. The normalized measurements obtained from different networks
455 agree within 48% for OC and 20% for EC, suggesting measurements from different networks can be
456 synchronized to generate harmonized carbonaceous concentration maps for constraining/verifying
457 climate model and for investigating emission sources and sinks. A North America harmonized
458 carbonaceous concentration map is useful for evaluating the national and inter-national mitigation
459 policies efforts on improving air quality and reducing fossil fuel consumption.

460 Carbon concentrations exhibited a non-linear positive dependency with ambient temperature,
461 and this relationship is characterized by a sigmoid function. Preliminary observations suggested that the
462 increases in OC and TC concentrations when ambient temperatures rose beyond 10 °C during summer,
463 is likely corresponding to the sum of SOA formation, influences of forest fires, and increased

anthropogenic activities. The moderate increase in EC concentration with increasing ambient temperature is believed to be a result of increased primary emissions from anthropogenic activities. The increase in OC concentration with temperature is consistent with the climate feedback mechanisms reported from various studies.

Nomenclature

AIHL	Air-industrial hygiene laboratory
AMS	Accelerator mass spectrometry
BC	Black carbon
CABM	Canadian Aerosol Baseline Measurement
CAPMoN	Canadian Air and Precipitation Monitoring Network
CARE	Center for Atmospheric Research Experiment
CCMR	Climate Chemistry Measurements and Research
DRI	Desert Research Institute
DRI-TOR	CAPMoN measurements using IMPROVE on DRI analyzer with TOR correction
EC	Elemental carbon
ECCC	Environment and Climate Change Canada
ECT9	EnCan-Total-900 protocol
FID	Flame ionization detector
FLEXPART	FLEXible PARTicle dispersion model
ICP	Inter-comparison study
IMPROVE	Interagency Monitoring PROtected Visual Environments
IMPROVE_A TOR	IMPROVE_A TOR protocol on DRI analyzer
KCCAMS	Keck Carbon Cycle accelerator mass spectrometry
MAC	Mass absorption coefficient
NIST	National Institute of Standard and Technology
OC	Organic carbon
PM	Particulate matter
POC	Pyrolyzed organic carbon
PSAP	Particle Soot Absorption Photometer
SOA	Secondary organic aerosol
SRM	Standard Reference Material
Sunset-TOT	IMPROVE TOT protocol on Sunset analyzer
TC	Total carbon
TEA	Thermal evolution analysis
TOA	Thermal optical analysis
TOR	Thermal optical reflectance
TOT	Thermal optical transmittance
UCI	University of California Irvine

Acknowledgements

Authors would like to acknowledge Elton Chan and Douglas Chan of ECCC for providing the FLEXPART model results and providing technical advice. IMPROVE measurements were obtained directly from the IMPROVE web site (http://vista.cira.colostate.edu/IMPROVE/Data/QA_QC/Advisory.htm). IMPROVE is a collaborative association of state, tribal, and federal agencies, and international partners. U.S. Environmental Protection Agency is the primary funding source, with contracting and research support from the National Park Service. IMPROVE carbon analysis was provided by Desert Research Institute. Funding of this study was initiated by Climate Change Technology and Innovation Initiative (CCTI) program, operated through Natural Resources Canada (NRCan), and supported by Clean Air Regulatory Agenda (CARA) initiative and ECCC internal federal funding.

Supplementary Information:

Additional details on thermal/optical analysis, the experimental parameters used in different temperature protocols (IMPROVE, IMPROVE_A, ECT9), radiocarbon analysis, vapor adsorption uncertainty, seasonality of carbonaceous measurements, wind rose analysis, and FLEXPART back trajectory analysis at Egbert are included in the Supplementary Information.

References:

Beverly, R.K., Beaumont, W., Tauz, D., Ormsby, K.M., von Reden, K.F., Santos, G.M. and Southon, J.R.: The Keck Carbon Cycle AMS Laboratory, University of California, Irvine: Status report, Radiocarbon 52, 301-309, 2010.

Birch, M. E. and Cary, R. A.: Elemental carbon-based method for monitoring occupational exposures to particulate diesel exhaust, Aerosol Sci. Technol., 25, 221-241, 1996.

Bond, T. C. and Bergstrom, R. W.: Light absorption by carbonaceous particles: An investigative review, Aerosol Sci. Technol., 40, 27-67, 2006.

Bond, T. C., Doherty, S. J., Fahey, D. W., Forster, P. M., Berntsen, T., DeAngelo, B. J., Flanner, M. G., Ghan, S., Karcher, B., Koch, D., Kinne, S., Kondo, Y., Quinn, P. K., Sarofim, M. C., Schultz, M. G., Schulz, M., Venkataraman, C., Zhang, H., Zhang, S., Bellouin, N., Guttikunda, S. K., Hopke, P. K., Jacobson, M. Z., Kaiser, J. W., Klimont, Z., Lohmann, U., Schwarz, J. P., Shindell, D., Storelvmo, T., Warren, S. G., and Zender, C. S.: Bounding the role of black carbon in the climate system: A scientific assessment, J. Geophys. Res. Atmos., 118, 5380-5552, 2013.

Cachier, H., Bremond, M. P., and Buat-Ménard, P.: Thermal separation of soot carbon, Aerosol Sci. Technol., 10, 358-364, 1989.

535 Cavalli, F., Viana, M., Yttri, K. E., Genberg, J., and Putaud, J. P.: Toward a standardized thermal-optical
536 protocol for measuring atmospheric organic and elemental carbon: The EUSAAR protocol, Atmos. Meas.
537 Tech., 3, 79-89, 2010.

538 Cavanagh, R. R. and Watters, Jr., R. L.: National Institute of Standards and Technology: Report of
539 Investigation Reference Material 8785: Air particulate matter on filter media (A fine fraction of SRM
540 1649a urban dust on quartz-fiber filter), 2005.

541 Chan, T. W. and Mozurkewich, M.: Application of absolute principal component analysis to size
542 distribution data: identification of particle origins, Atmos. Chem. Phys, 7, 887-897, 2007.

543 Chan, T. W., Huang, L., Leaitch, W. R., Sharma, S., Brook, J. R., Slowik, J. G., Abbatt, J. P. D., Brickell, P. C.,
544 Liggio, J., Li, S. M., and Moosmüller, H.: Observations of OM/OC and specific attenuation coefficients
545 (SAC) in ambient fine PM at a rural site in central Ontario, Canada, Atmos. Chem. Phys, 10, 2393-2411,
546 2010.

547 Chen, L.-W. A., Chow, J. C., Watson, J. G., Moosmüller, H., and Arnott, W. P.: Modeling reflectance and
548 transmittance of quartz-fiber filter samples containing elemental carbon particles: Implications for
549 thermal/optical analysis, J. Aerosol Sci., 35, 765-780, 2004.

550 Chen, L.-W. A., Chow, J. C., Watson, J. G., and Schichtel, B. A.: Consistency of long-term elemental
551 carbon trends from thermal and optical measurements in the IMPROVE network, Atmos. Meas. Tech., 5,
552 2329-2338, 2012.

553 Chow, J. C., Watson, J. G., Pritchett, L. C., Pierson, W. R., Frazier, C. A., and Purcell, R. G.: The DRI
554 Thermal/Optical Reflectance carbon analysis system: Description, evaluation and applications in U.S. air
555 quality studies, Atmos. Environ., 27A, 1185-1201, 1993.

556 Chow, J. C., Watson, J. G., Crow, D., Lowenthal, D. H., and Merrifield, T. M.: Comparison of IMPROVE and
557 NIOSH carbon measurements, Aerosol Sci. Technol., 34, 23-34, 2001.

558 Chow, J. C., Watson, J. G., Chen, L.-W. A., Arnott, W. P., Moosmüller, H., and Fung, K. K.: Equivalence of
559 elemental carbon by Thermal/Optical Reflectance and Transmittance with different temperature
560 protocols, Environ. Sci. Technol., 38, 4414-4422, 2004.

561 Chow, J. C., Watson, J. G., Louie, P. K. K., Chen, L.-W. A., and Sin, D.: Comparison of $PM_{2.5}$ carbon
562 measurement methods in Hong Kong, China, Environ. Poll, 137, 334-344, 2005.

563 Chow, J. C., Watson, J. G., Chen, L.-W. A., Chang, M.-C. O., Robinson, N. F., Trimble, D. L., and Kohl, S. D.:
564 The IMPROVE_A temperature protocol for thermal/optical carbon analysis: Maintaining consistency
565 with a long-term database, J. Air Waste Manage. Assoc., 57, 1014-1023, 2007.

566 Chow, J. C., Watson, J. G., Lowenthal, D. H., and Chen, L.-W. A.: Climate change - Characterization of
567 black carbon and organic carbon air pollution emissions and evaluation of measurement methods Phase
568 II: Characterization of black carbon and organic carbon source emissions, Desert Research Institute,
569 Reno, NVDRI 04-307, 2009.

570 Chow, J. C., Bachmann, J. D., Kinsman, J. D., Legge, A. H., Watson, J. G., Hidy, G. M., and Pennell, W. R.:
571 Multipollutant air quality management: Critical review discussion, J. Air Waste Manage. Assoc., 60,
572 1151-1164, 2010.

573 Collaud-Coen, M. C., Andrews, E., Asmi, A., Baltensperger, U., Bukowiecki, N., Day, D., Fiebig, M.,
574 Fjaeraa, A. M., Flentje, H., Hyvarinen, A., Jefferson, A., Jennings, S. G., Kouvarakis, G., Lihavainen, H.,
575 Myhre, C. L., Malm, W. C., Mihapopoulos, N., Molenar, J. V., O'Dowd, C., Ogren, J. A., Schichtel, B. A.,
576 Sheridan, P., Virkkula, A., Weingartner, E., Weller, R., and Laj, P.: Aerosol decadal trends - Part 1: In-situ
577 optical measurements at GAW and IMPROVE stations, Atmos. Chem. Phys, 13, 869-894, 2013.

578 Countess, R. J.: Interlaboratory analyses of carbonaceous aerosol samples, Aerosol Sci. Technol., 12, 114-
579 121, 1990.

580 Currie, L. A., Benner, B. A., Jr., Cachier, H., Cary, R., Chow, J. C., Druffel, E. R. M., Eglinton, T. I.,
581 Gustafsson, Ö., Hartmann, P. C., Hedges, J. I., Kessler, J. D., Kirchstetter, T. W., Klinedinst, D. B., Klouda,
582 G. A., Marolf, J. V., Masiello, C. A., Novakov, T., Pearson, A., Prentice, K. M., Puxbaum, H., Quinn, J. G.,
583 Reddy, C. M., Schmid, H., Slater, J. F., Watson, J. G., and Wise, S. A.: A critical evaluation of
584 interlaboratory data on total, elemental, and isotopic carbon in the carbonaceous particle reference
585 material, NIST SRM 1649a, Journal of Research of the National Institute of Standards and Technology,
586 107, 279-298, 2002.

587 Ding, L., Chan, T. W., Ke, F. and Wang, D. K. W.: Characterization of chemical composition and
588 concentration of fine particulate matter during a transit strike in Ottawa, Canada, Atmos. Environ., 89,
589 433-442, 2014.

590 Flagan, R. C. and Seinfeld, J. H.: Fundamentals of Air Pollution Engineering, Prentice Hall, Englewood
591 Cliffs, NJ, 1988.

592 Fuller, K. A., Malm, W. C., and Kreidenweis, S. M.: Effects of mixing on extinction by carbonaceous
593 particles, Journal of Geophysical Research, 104, 15941-15954, 1999.

594 Fung, K. K.: Particulate carbon speciation by MnO2 oxidation, Aerosol Sci. Technol., 12, 122-127, 1990.

595 Han, Y. M., Cao, J. J., An, Z., Chow, J. C., Watson, J. G., Jin, Z. D., Fung, K. K., and Liu, S.: Evaluation of the
596 thermal/optical reflectance method for quantification of elemental carbon in sediments, Chemosphere,
597 69, 526-533, 2007.

598 Healy, R. M., Sofowote, U., Su, Y., Debosz, J., Noble, M., Jeong, C. H., Wang, J. M., Hilker, N., Evans, G. J.,
599 Doerksen, G., Jones, K., and Munoz, A.: Ambient measurements and source apportionment of fossil fuel
600 and biomass burning black carbon in Ontario, Atmos. Environ., 161, 34-47, 2017.

601 Hinds, W. C.: Straight-line acceleration and curvilinear particle motion. In: Aerosol Technology.
602 Properties, Behavior, and Measurement of airborne Particles, 2nd Ed., John Wiley & Sons, Inc., New
603 York, 1999.

604 Huang, L., Brook, J. R., Zhang, W., Li, S. M., Graham, L., Ernst, D., Chivulescu, A., and Lu, G.: Stable
605 isotope measurements of carbon fractions (OC/EC) in airborne particulate: A new dimension for source
606 characterization and apportionment, Atmos. Environ., 40, 2690-2705, 2006.

607 Huntzicker, J. J., Johnson, R. L., Shah, J. J., and Cary, R. A.: Analysis of organic and elemental carbon in
608 ambient aerosols by a thermal-optical method. In: Particulate Carbon: Atmospheric Life Cycle, Wolff, G.
609 T. and Klimisch, R. L. (Eds.), Plenum Press, New York, NY, 1982.

610 IMPROVE: Interagency Monitoring of Protected Visual Environments, National Park Service, Ft. Collins,
611 CO, 2017.

612 Japar, S. M., Brachaczek, W. W., Gorse, R. A., Jr., Norbeck, J. H., and Pierson, W. R.: The contribution of
613 elemental carbon to the optical properties of rural atmospheric aerosols, Atmos. Environ., 20, 1281-
614 1289, 1986.

615 Khalek, I. A.: 2007 diesel particulate measurement research, Coordinating Research Council, Alpharetta,
616 GA, 2008.

617 Kittelson, D. B.: Engines and nanoparticles: A review, J. Aerosol Sci., 29, 575-588, 1998.

618 Klouda, G. A., Filliben, J. J., Parish, H. J., Chow, J. C., Watson, J. G., and Cary, R. A.: Reference material
619 8785: Air particulate matter on filter media, Aerosol Sci. Technol., 39, 173-183, 2005.

620 Lavoué, D., Liousse, C., Cachier, H., Stocks, B. J., and Goldammer, J. G.: Modeling of carbonaceous
621 particles emitted by boreal and temperate wildfires at northern latitudes, J. Geophys. Res. Atmos., 105,
622 26871-26890, 2000.

623 Leaitch, W. R., MacDonald, A. M., Brickell, P. C., Liggio, J., Sjostedt, S. J., Vlasenko, A., Bottenheim, J. W.,
624 Huang, L., Li, S. M., Liu, P. S. K., Toom-Sauntry, D., Hayden, K. A., Sharma, S., Shantz, N. C., Wiebe, H. A.,
625 Zhang, W., Abbatt, J. P. D., Slowik, J. G., Chang, R. Y. W., Russell, L. M., Schwartz, R. E., Takahama, S.,
626 Jayne, J. T., Ng, N. L.: Temperature response of the submicron organic aerosol from temperate forests,
627 Atmos. Environ., 45, 6696-6704, 2011.

628 Lesins, G., Chylek, P., and Lohmann, U.: A study of internal and external mixing scenarios and its effect
629 on aerosol optical properties and direct radiative forcing, J. Geophys. Res., 107, 4904,
630 10.1029/2001JD000973, 2002.

631 Malm, W. C.: Atmospheric haze: Its sources and effects on visibility in rural areas of the continental
632 United States, Env. Mon. Ass., 12, 203-225, 1989.

633 Malm, W. C., Sisler, J. F., Huffman, D., Eldred, R.A., and Cahill, T. A.: Spatial and seasonal trends in
634 particle concentration and optical extinction in the United States, J. Geophys. Res., 99, 1347-1370, 1994.

635 May, W. E. and Trahey, N. M.: National Institute of Standards and Technology: Certificate of Analysis
636 Standard Reference Material 1649a: Urban dust, 2001.

637 McDow, S. R. and Huntzicker, J. J.: Vapor adsorption artifact in the sampling of organic aerosol: Face
638 velocity effects, Atmos. Environ., 24A, 2563-2571, 1990.

639 Paasonen, P., Asmi, A., Petäjä, T., Kajos, M. K., Äijälä, M., Junninen, H., Holst, T., Abbatt, J. P. D., Arneth,
640 A., Birmili, W., van der Gon, H. D., Hamed, A., Hoffer, A., Laakso, L., Laaksonen, A., Leaitch, W. R., Plass-
641 Dülmer, C., Pryor, S. C., Räisänen, P., Swietlicki, E., Wiedensohler, A., Worsnop, D. R., Kerminen, V. M.,
642 and Kulmala, M.: Warming-induced increase in aerosol number concentration likely to moderate climate
643 change, Nature Geoscience, 6, 438-442, 2013.

644 Petzold, A., Ogren, J. A., Fiebig, M., Laj, P., Li, S. M., Baltensperger, U., Holzer-Popp, T., Kinne, S.,
645 Pappalardo, G., Sugimoto, N., Wehrli, C., Wiedensohler, A., and Zhang, X. Y.: Recommendations for
646 reporting "black carbon" measurements, Atmos. Chem. Phys, 13, 8365-8379, 2013.

647 Rupakheti, M., Leaitch, W. R., Lohmann, U., Hayden, K., Brickell, P., Lu, G., Li, S. M., Toom-Sauntry, D.,
648 Bottenheim, J. W., Brook, J. R., Vet, R., Jayne, J. T., and Worsnop, D. R.: An intensive study of the size and

composition of submicron atmospheric aerosols at a rural site in Ontario, Canada, Aerosol Sci. Technol., 39, 722-736, 2005.

Santos, G.M., Moore, R., Southon, J., Griffin, S., Hinger, E., Zhang, D.: AMS 14C preparation at the KCCAMS/UCI Facility: Status report and performance of small samples. Radiocarbon, 49, 255-269, 2007.

Schulz, M., Textor, C., Kinne, S., Balkanski, Y., Bauer, S., Berntsen, T., Berglen, T., Boucher, O., Dentener, F., Guibert, S., Isaksen, I. S. A., Iversen, T., Koch, D., Kirkevag, A., Liu, X., Montanaro, V., Myhre, G., Penner, J. E., Pitari, G., Reddy, S., Seland, O., Stier, P., and Takemura, T.: Radiatives forcing by aerosols as derived from the AeroCom present-day and pre-industrial simulations, Atmos. Chem. Phys, 6, 5225-5246, 2006.

Schwarz, J. P., Gao, R. S., Fahey, D. W., Thomson, D. S., Watts, L. A., Wilson, J. C., Reeves, J. M., Darbeheshti, M., Baumgardner, D. G., Kok, G. L., Chung, S. H., Schulz, M., Hendricks, J., Lauer, A., Kärcher, B., Slowik, J. G., Rosenlof, K. H., Thompson, T. L., Langford, A. O., Loewenstein, M., and Aikin, K.C.: Single-particle measurements of midlatitude black carbon and light-scattering aerosols from the boundary layer to the lower stratosphere, J. Geophys. Res., 111, D16207, doi:10.1029/2006JD007076, 2006.

Slowik, J. G., Stroud, C., Bottenheim, J. W., Brickell, P. C., Chang, R. Y. W., Liggio, J., Makar, P. A., Martin, R. V., Moran, M. D., Shantz, N. C., Sjostedt, S. J., van Donkelaar, A., Vlasenko, A., Wiebe, H. A., Xia, A. G., Zhang, J., Leaitch, W. R., and Abbatt, J. P. D.: Characterization of a large biogenic secondary organic aerosol event from eastern Canadian forests, Atmos. Chem. Phys, 10, 2825-2845, 2010.

Stohl, A., Forster, C., Frank, A., Seibert, P., and Wotawa, G.: Technical note: The Lagrangian particle dispersion model FLEXPART version 6.2, Atmos. Chem. Phys, 5, 2461-2474, 2005.

Sutter, B., Bemer, D., Appert-Collin, J. C., Thomas, D., and Midoux, N.: Evaporation of liquid semi-volatile aerosols collected on fibrous filters, Aerosol Sci. Technol., 44, 395-404, 2010.

Tunved, P., Hansson, H. C., Kerminen, V. M., Strom, J., Dal Maso, M., Lihavainen, H., Viisanen, Y., Aalto, P. P., Komppula, M., and Kulmala, M.: High natural aerosol loading over boreal forests, Science, 312, 261-263, 2006.

Turpin, B. J., Huntzicker, J. J., and Hering, S. V.: Investigation of organic aerosol sampling artifacts in the Los Angeles Basin, Atmos. Environ., 28, 3061-3071, 1994.

Viana, M., Chi, X., Maenhaut, W., Cafmeyer, J., Querol, X., Alastuey, A., Mikuska, P., and Vecera, Z.: Influence of sampling artefacts on measured PM, OC, and EC levels in carbonaceous aerosols in an urban area, Aerosol Sci. Technol., 40, 107-117, 2006.

Watson, J. G., Chow, J. C., Shah, J. J., and Pace, T. G.: The effect of sampling inlets on the PM_{10} and PM_{15} to TSP concentration ratios, J. Air Pollut. Control Assoc., 33, 114-119, 1983.

Watson, J. G.: Critical review: Visibility: Science and regulation, J. Air Waste Manage. Assoc., 52, 628-713, 2002.

Watson, J. G., Chow, J. C., and Chen, L.-W. A.: Summary of organic and elemental carbon/black carbon analysis methods and intercomparisons, Aerosol Air Qual. Res., 5, 65-102, 2005.

686 Watson, J. G., Chow, J. C., Chen, L. W. A., and Frank, N. H.: Methods to assess carbonaceous aerosol
687 sampling artifacts for IMPROVE and other long-term networks, J. Air & Waste Manage. Assoc., 59, 898-
688 911, 2009.

689 Watson, J. G., Chow, J. C., Chen, L.-W. A., and Wang, X. L.: Measurement system evaluation for fugitive
690 dust emissions detection and quantification, Desert Research Institute, Reno, NV, 2010.

691 Watson, J. G., and Chow, J. C.: Ambient aerosol sampling in: Aerosol Measurement: Principles,
692 techniques and applications, Third Edition, edited by Kulkarni, P., Baron, P.A., and Willeke, K., pp. 591-
693 614, Hoboken, NJ, USA: Wiley, 2011.

694 Yang, F., Huang, L., Sharma, S., Brook, J. R., Zhang, W., Li, S. M., and Tan, J. H.: Two-year observations of
695 fine carbonaceous particles in variable sampling intervals, Atmos. Environ., 45, 2418-2426, 2011.

696 Yang, H. and Yu, J. Z.: Uncertainties in charring correction in the analysis of elemental and organic
697 carbon in atmospheric particles by thermal/optical methods, Environ. Sci. Technol., 36, 5199-5204,
698 2002.

699 Yu, S. C., Dennis, R. L., Bhave, P. V., and Eder, B. K.: Primary and secondary organic aerosols over the
700 United States: Estimates on the basis of observed organic carbon (OC) and elemental carbon (EC), and
701 air quality modeled primary OC/EC ratios, Atmos. Environ., 38, 5257-5268, 2004.

Atmos. Meas. Tech. Discuss., https://doi.org/10.5194/amt-2019-104
Manuscript under review for journal Atmos. Meas. Tech.
Discussion started: 18 April 2019

Atmospheric Measurement Techniques Discussions

Table 1 Specifications for the filter sampling systems used by the three networks.

	IMPROVE	CAPMoN		CABM
Data coverage period	2005-2015	2005-2007	2008-2015	2005-2015
Analytical instrument	DRI	Sunset	DRI	Sunset
Thermal/optical protocol	IMPROVE_A	IMPROVE	IMPROVE	ECT9
Pyrolyzed organic carbon detection	Reflect.	Transmit.	Reflect. & Transmit.	Retention time
Particle size selection method	Cyclone	Impactor plates	Impactor plates	Cyclone
Particle size cut off diameter (nm)	2.5	2.5	2.5	2.5
Sampling flow rate (L/min)	22.8	10.0	10.0	16.7
Filter media model	2500QAT-UP	2500QAT-UP	2500QAT-UP	2500QAT-UP
Quartz filter diameter (mm)	25	47	47	47
Filter deposition exposure area (cm^2)	3.53	10.75	10.75	13.85
Filter face velocity (cm/s)	107.65	15.50	15.50	20.09
Sampling frequency	Daily every 3 days	Daily every 3 days	Daily every 3 days	Integrated weekly
Daily sampled air volume (L/day)	31680	14400	14400	24048
Air volume per sample (m^3)	31.68	14.4	14.4	168.3
Positive artifact correction	Yes	Yes	Yes	No
Filter blank correction	Yes	No	No	Yes

Atmos. Meas. Tech. Discuss., https://doi.org/10.5194/amt-2019-104
Manuscript under review for journal Atmos. Meas. Tech.
Discussion started: 18 April 2019

Atmospheric Measurement Techniques Discussions

Table 2 Regression results (slope, correlation coefficient, and total number of points) obtained when fitting various CABM (ECT9) and CAPMoN (Sunset-TOT & DRI-TOR) carbonaceous mass concentration time series against IMPROVE (IMPROVE_A TOR) measurements. IMPROVE_A TOR and ECT9 measurements cover the period from 2005 to 2015. Sunset-TOT and DRI-TOR measurements cover the periods for 2005-2008 and 2008-2015, respectively. Regression 1 indicates the best-fitted slope through the origin. Regression 2 is the best-fitted slope with intercept (in brackets).

	Regression 1	Regression 2	R	N
Sunset-TOT TC vs IMPROVE_A TOR TC	0.888±0.033	0.713±0.112 (0.301±0.186)	0.78	28
Sunset-TOT OC vs IMPROVE_A TOR OC	0.967±0.041	0.873±0.135 (0.125±0.170)	0.79	28
Sunset-TOT EC vs IMPROVE_A TOR EC	0.639±0.042	0.233±0.130 (0.171±0.053)	0.33	28
Sunset-TOT POC vs IMPROVE_A TOR POC	1.769±0.091	1.776±0.351 (-0.003±0.127)	0.70	28
DRI-TOR TC vs IMPROVE_A TOR TC	0.832±0.015	0.946±0.044 (-0.164±0.059)	0.91	93
DRI-TOR OC vs IMPROVE_A TOR OC	0.835±0.017	0.934±0.046 (-0.116±0.050)	0.90	93
DRI-TOR EC vs IMPROVE_A TOR EC	0.818±0.019	0.929±0.072 (-0.032±0.020)	0.81	93
DRI-TOR POC vs IMPROVE_A TOR POC	0.986±0.028	1.230±0.080 (-0.073±0.023)	0.85	93
ECT9 TC vs IMPROVE_A TOR TC	1.304±0.022	1.197±0.065 (0.164±0.093)	0.88	107
ECT9 OC vs IMPROVE_A TOR OC	1.149±0.021	1.004±0.056 (0.179±0.064)	0.87	107
ECT9 EC vs IMPROVE_A TOR EC	1.834±0.046	1.661±0.149 (0.056±0.046)	0.74	107
ECT9 POC vs IMPROVE_A TOR POC	0.998±0.031	0.615±0.082 (0.124±0.025)	0.59	107

Atmos. Meas. Tech. Discuss., https://doi.org/10.5194/amt-2019-104
Manuscript under review for journal Atmos. Meas. Tech.
Discussion started: 18 April 2019

Atmospheric Measurement Techniques Discussions

713 **Table 3** Correlation coefficients (r) of various *normalized* carbonaceous mass measurements among different networks (IMPROVE, CAPMoN and
714 CABM). All measurements cover the period from 2008 to 2015.

		IMPROVE_A TOR				DRI-TOR				ECT9			
		TC	OC	EC	POC	TC	OC	EC	POC	TC	OC	EC	POC
IMPROVE_A TOR	TC	1	0.99	0.80	0.91	0.91	0.91	0.68	0.87	0.86	0.86	0.77	0.50
	OC		1	0.73	0.91	0.90	0.90	0.63	0.87	0.86	0.86	0.74	0.50
	EC			1	0.71	0.76	0.70	0.81	0.69	0.71	0.65	0.75	0.37
	POC				1	0.82	0.81	0.62	0.85	0.82	0.79	0.77	0.46
DRI-TOR	TC					1	0.99	0.74	0.92	0.79	0.78	0.71	0.41
	OC						1	0.64	0.92	0.77	0.77	0.67	0.40
	EC							1	0.63	0.63	0.56	0.69	0.31
	POC								1	0.77	0.75	0.70	0.44
ECT9	TC									1	0.98	0.91	0.58
	OC										1	0.82	0.65
	EC											1	0.37
	POC												1

715

716 **Table 4** Regression results (slope, correlation coefficient, and total number of points) obtained when fitting various CABM (ECT9)and CAPMoN
717 (Sunset-TOT & DRI-TOR) *normalized* carbonaceous mass concentration time series against IMPROVE (IMPROVE_A TOR) measurements. All
718 measurement sets cover the period from 2008 to 2015. Regression 1 indicates the best-fitted slope through the origin. Regression 2 is the best-
719 fitted slope with intercept (in brackets).

	Regression 1	Regression 2	R	N
DRI-TOR TC vs IMPROVE_A TOR TC	1.238±0.022	1.408±0.065 (-0.192±0.069)	0.91	93
DRI-TOR OC vs IMPROVE_A TOR OC	1.322±0.027	1.479±0.073 (-0.193±0.084)	0.90	93
DRI-TOR EC vs IMPROVE_A TOR EC	1.033±0.024	1.173±0.090 (-0.126±0.078)	0.81	93
DRI-TOR POC vs IMPROVE_A TOR POC	1.280±0.036	1.597±0.104 (-0.296±0.092)	0.85	93
ECT9 TC vs IMPROVE_A TOR TC	0.804±0.016	0.7136±0.045 (0.104±0.049)	0.86	86
ECT9 OC vs IMPROVE_A TOR OC	0.711±0.015	0.591±0.038 (0.151±0.044)	0.86	86
ECT9 EC vs IMPROVE_A TOR EC	1.125±0.030	1.198±0.114 (-0.066±0.100)	0.75	86
ECT9 POC vs IMPROVE_A TOR POC	0.556±0.020	0.221±0.047 (0.318±0.042)	0.46	86

720

Atmos. Meas. Tech. Discuss., https://doi.org/10.5194/amt-2019-104
Manuscript under review for journal Atmos. Meas. Tech.
Discussion started: 18 April 2019

Atmospheric Measurement Techniques Discussions

721 **Figure 1** Comparison of: (a) TC, (b) OC, and (c) EC concentrations obtained from the same NIST SRM
722 8785 filters reported by ECCC following the TEA (ECT9) method and by DRI following the IMPROVE_A
723 protocol during the inter-comparison study in 2009/2010.

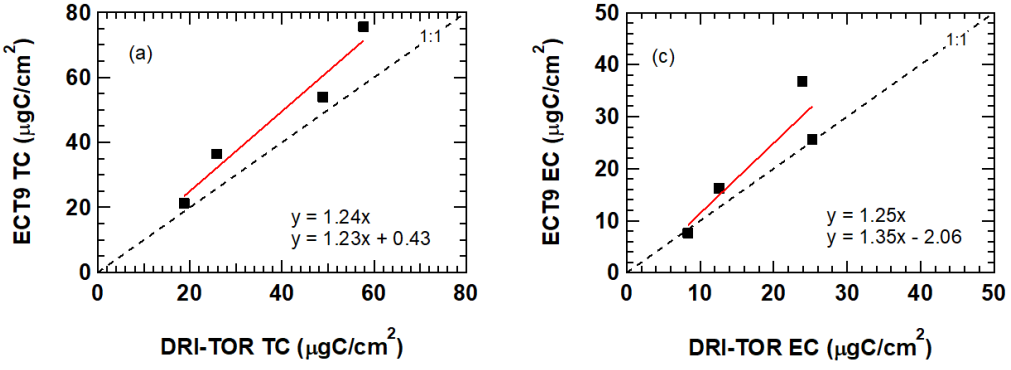

724

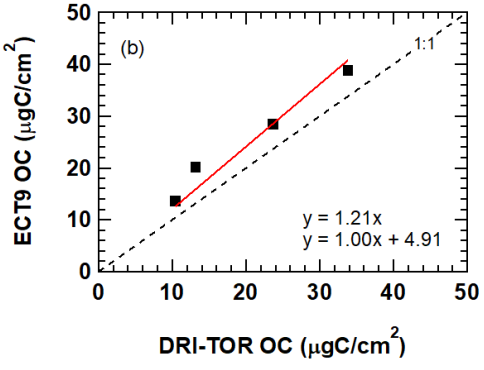

725

726

727

Atmos. Meas. Tech. Discuss., https://doi.org/10.5194/amt-2019-104
Manuscript under review for journal Atmos. Meas. Tech.
Discussion started: 18 April 2019

Atmospheric Measurement Techniques Discussions

728 **Figure 2** Comparison of the TC, OC, and EC measurements of the NIST SRM samples reported by the
729 ECCC and DRI groups during the inter-comparison study conducted between 2009 and 2010.
730 "Reported" represent the published value in the NIST SRM certificate (Cavanagh and Watters, 2005).
731 Error bars represent uncertainties covering 95% confidence interval. In (d), the ECT9 value (in green)
732 represents the calculated EC/TC ratio determined based on stable carbon isotope measurement
733 obtained from the SRM 1649a sample (Currie et al., 2002).

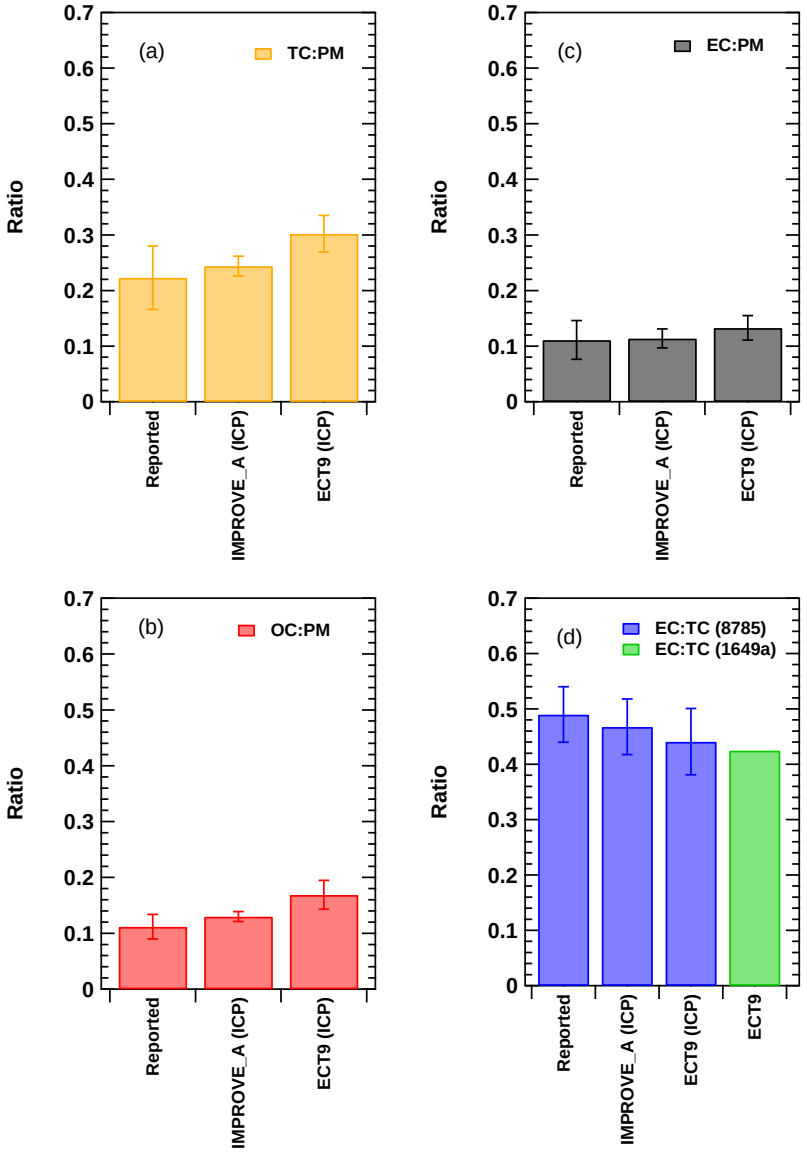

734

Atmos. Meas. Tech. Discuss., https://doi.org/10.5194/amt-2019-104
Manuscript under review for journal Atmos. Meas. Tech.
Discussion started: 18 April 2019

Atmospheric Measurement Techniques Discussions

735 **Figure 3** (a) Real-time Particle Soot Absorption Photometer (PSAP) measurements averaged to match
736 the corresponding sampling frequencies used in different networks. (b) Monthly PSAP measurements
737 derived from (a). (c) Comparison of the different sets of measurements from (b) with the 1:1 line shown
738 in red.

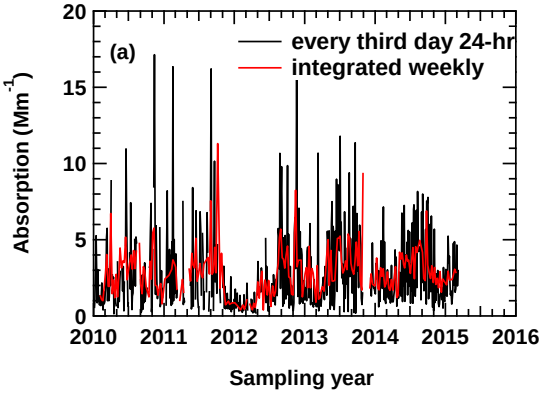

739

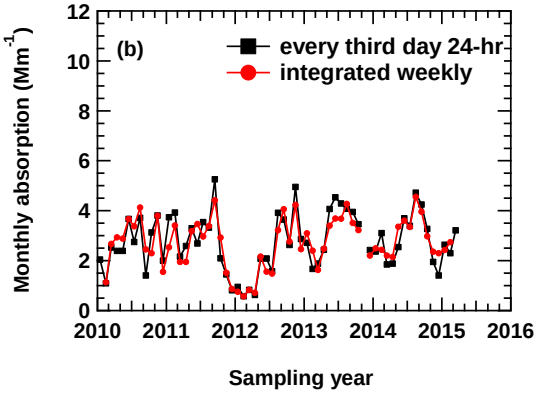

740

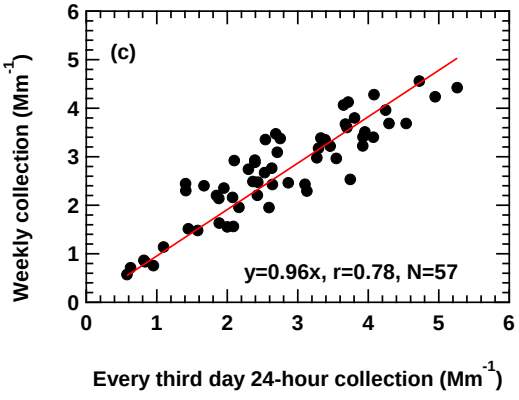

741

742

Atmos. Meas. Tech. Discuss., https://doi.org/10.5194/amt-2019-104
Manuscript under review for journal Atmos. Meas. Tech.
Discussion started: 18 April 2019

Atmospheric Measurement Techniques Discussions

743 **Figure 4** Monthly averaged CAPMoN (a) OC, (b) EC, and (c) POC mass concentration time series with and
744 without vapor adsorption correction. Note that the y-axes in Figures 4b and 4c are on different scale.

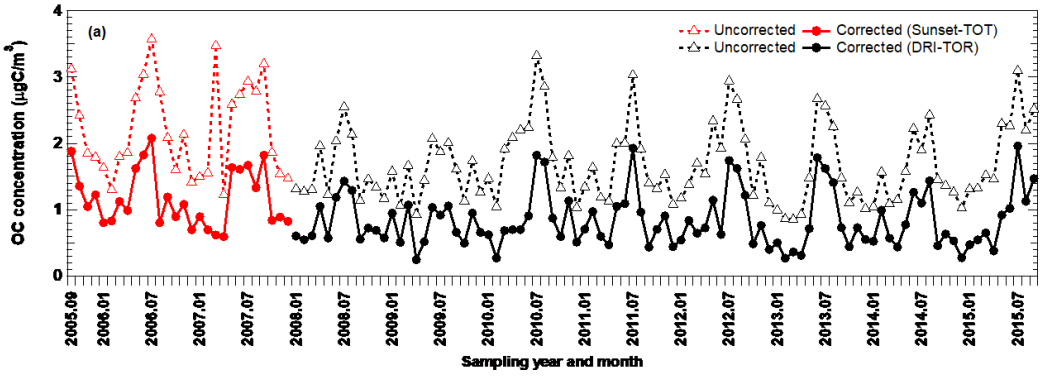

745

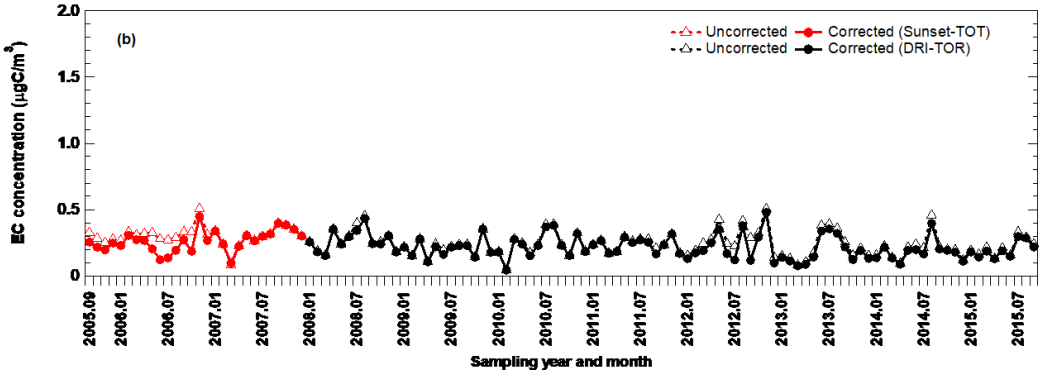

746

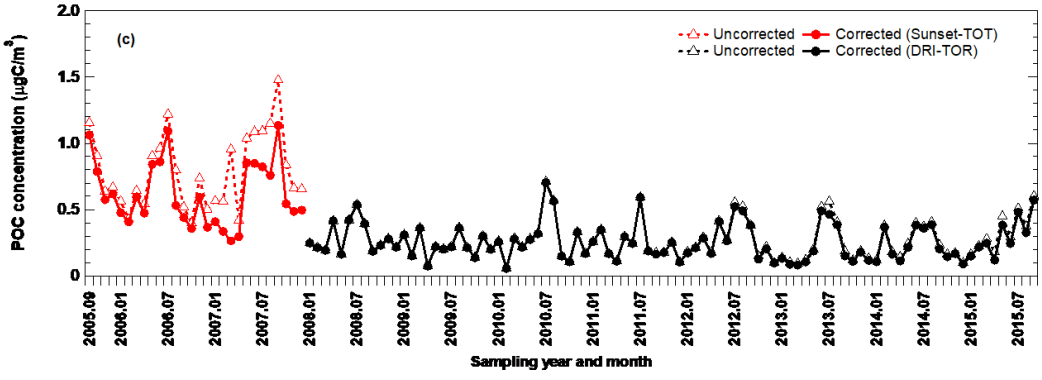

747

748

749

Atmos. Meas. Tech. Discuss., https://doi.org/10.5194/amt-2019-104
Manuscript under review for journal Atmos. Meas. Tech.
Discussion started: 18 April 2019

Atmospheric Measurement Techniques Discussions

750 **Figure 5** Relationship between the monthly averaged CAPMoN vapor adsorption corrected and
751 uncorrected measurements for (a) TC, (b) OC, (c) EC, and (d) POC. Black solid markers represent the TOR
752 measurements (2008-2015) analyzed by the DRI analyzer (i.e., DRI-TOR). Red open markers represent
753 the TOT measurements before 2008 analyzed by the Sunset analyzer (i.e., Sunset-TOT). The red line
754 represents the best-fitted linear regression of all the DRI-TOR measurements through the origin. All the
755 corresponding statistics (i.e., best-fitted slope, correlation coefficient, total number of measurement
756 points) are included in the legend.

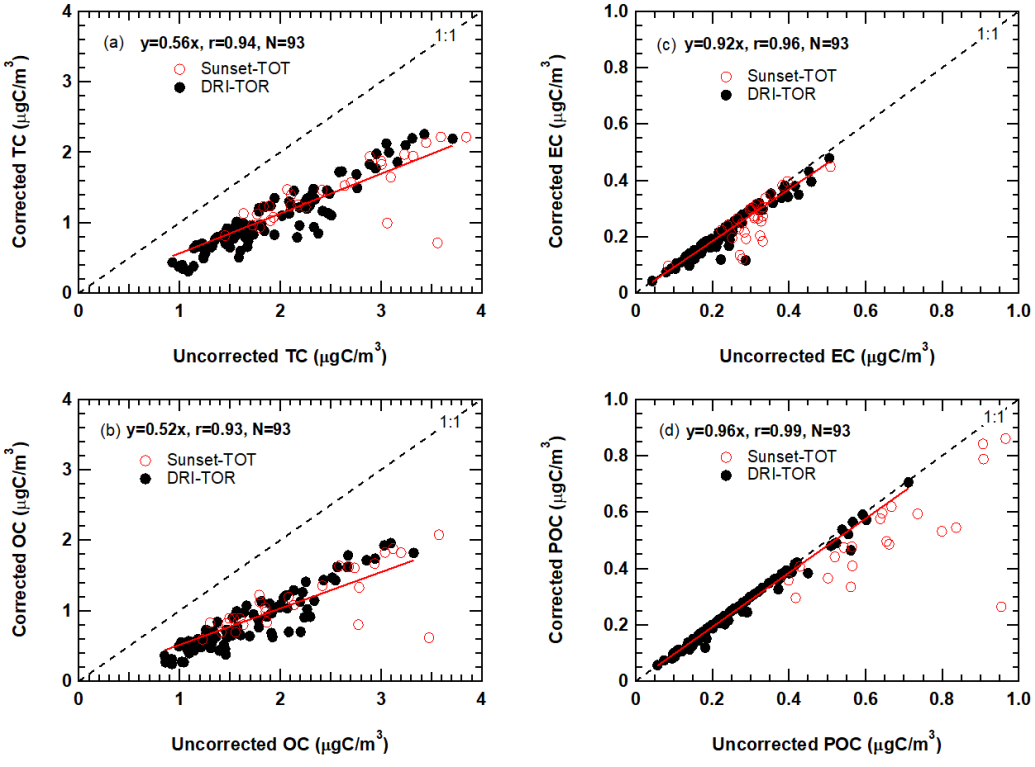

757

758

759

Atmos. Meas. Tech. Discuss., https://doi.org/10.5194/amt-2019-104
Manuscript under review for journal Atmos. Meas. Tech.
Discussion started: 18 April 2019

Atmospheric Measurement Techniques Discussions

760 **Figure 6** Monthly averaged (a) TC, (b) OC, (c) EC, and (d) POC concentration time series obtained from
761 three different networks. CAPMoN measurements before 2008 were obtained using Sunset-TOT
762 method (in green) while measurements starting 2008 were obtained using DRI-TOR method (in orange).

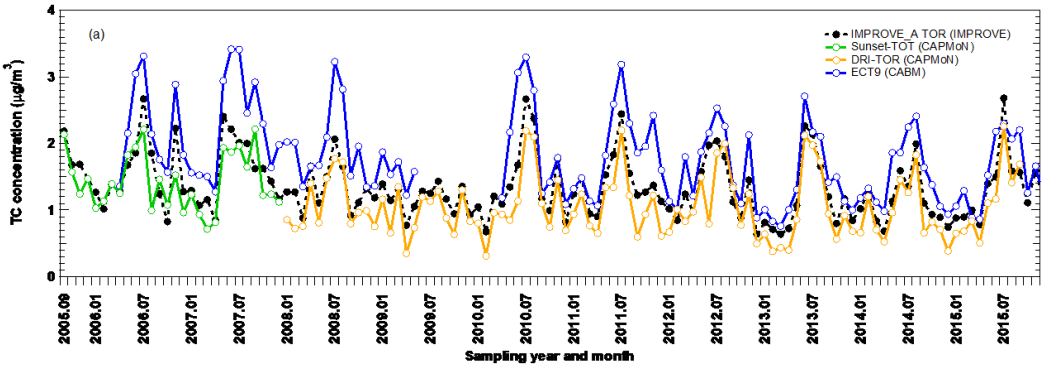

763

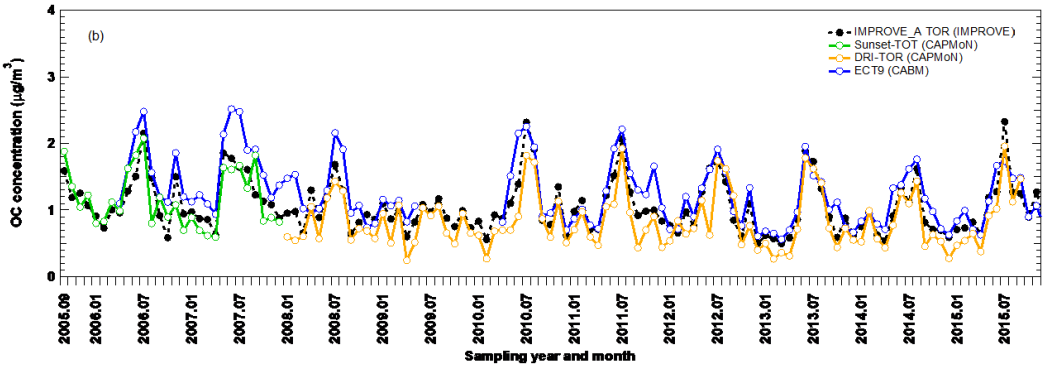

764

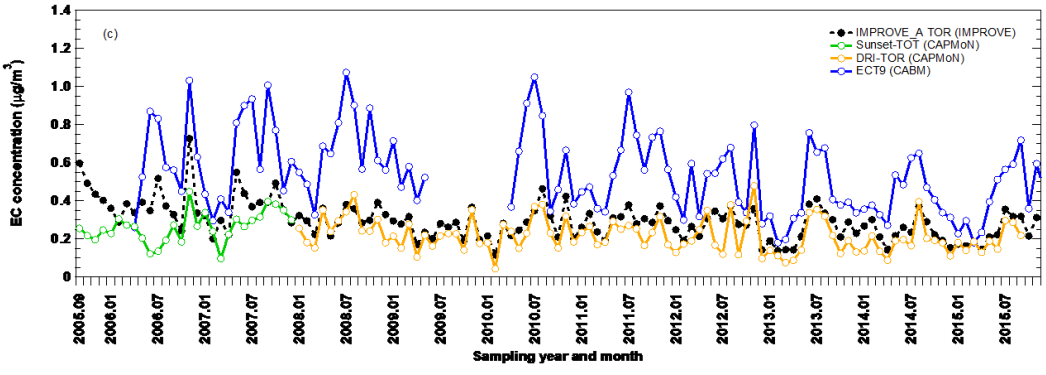

765

Atmos. Meas. Tech. Discuss., https://doi.org/10.5194/amt-2019-104
Manuscript under review for journal Atmos. Meas. Tech.
Discussion started: 18 April 2019

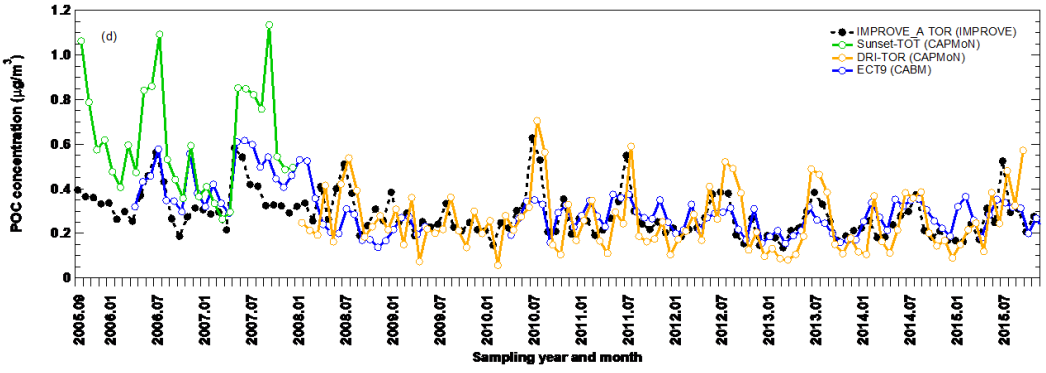

766

767

768

Atmos. Meas. Tech. Discuss., https://doi.org/10.5194/amt-2019-104
Manuscript under review for journal Atmos. Meas. Tech.
Discussion started: 18 April 2019

Atmospheric Measurement Techniques Discussions

769 **Figure 7** Comparison of the monthly averaged carbonaceous mass concentrations from the CAPMoN
770 (red circles and orange triangles) and CABM (black squares) networks against IMPROVE. The different
771 straight lines represent the linear regression best fitted line through the origin (i.e., Regression 1). The
772 fitted parameters for all corresponding data sets with (Regression 2) and without (Regression 1) the
773 y-intercept are summarized in Table 2.

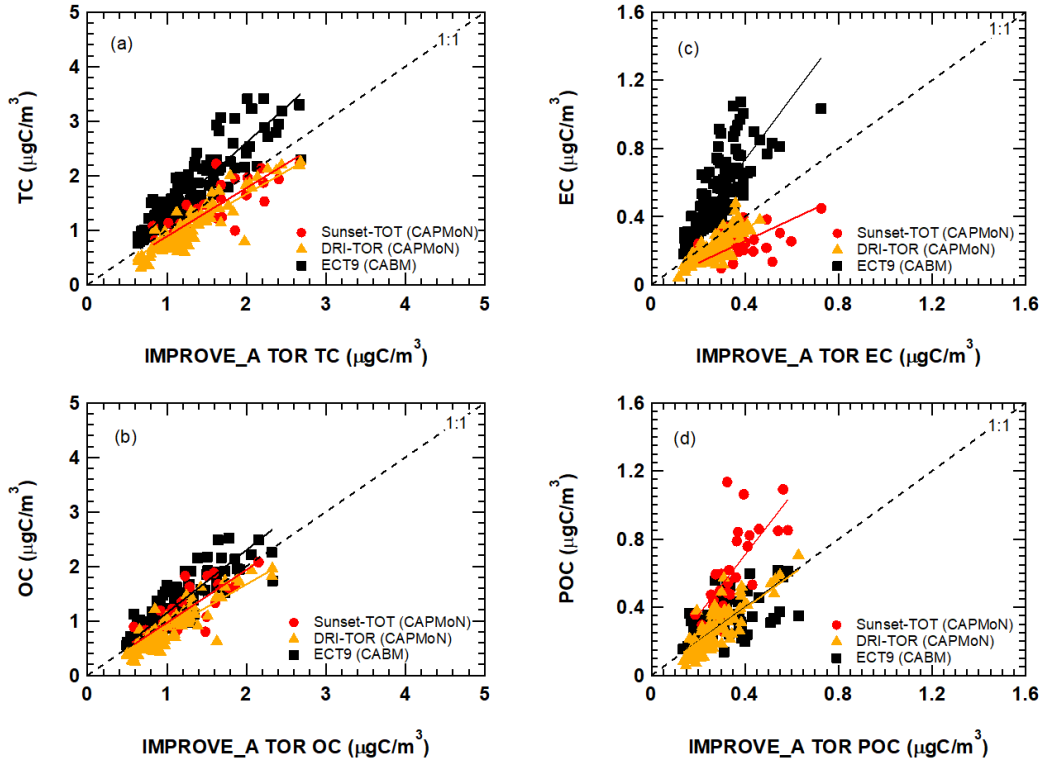

774

Atmos. Meas. Tech. Discuss., https://doi.org/10.5194/amt-2019-104
Manuscript under review for journal Atmos. Meas. Tech.
Discussion started: 18 April 2019

Atmospheric Measurement Techniques Discussions

775 **Figure 8** Normalized monthly averaged time series for (a) TC, (b) OC, (c) EC, and (d) POC for the
776 IMPROVE (black circles), CAPMoN (orange triangles), and CABM (blue squares) networks. All
777 measurements were normalized to their corresponding 2008 January mass concentration. Monthly
778 averaged ambient temperature in green dotted curve. Monthly averaged wind direction and speed (in
779 wind barb) are in red.

780

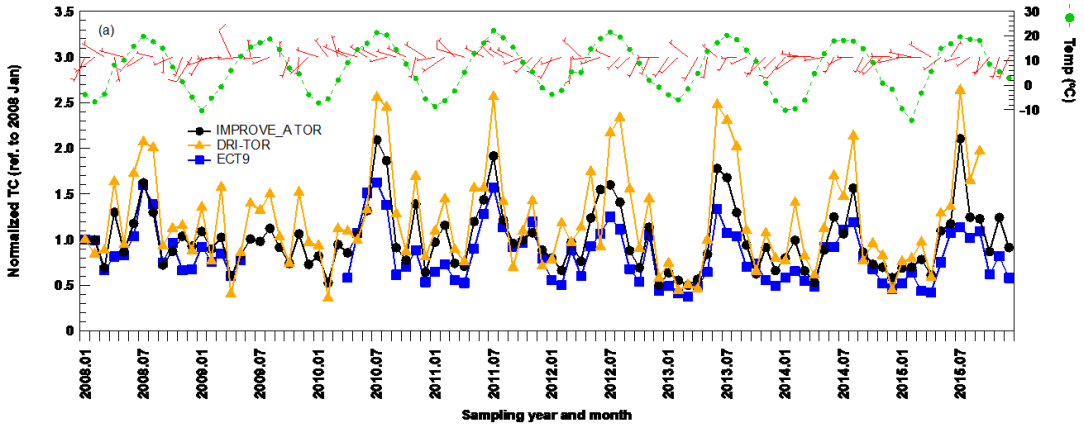

781

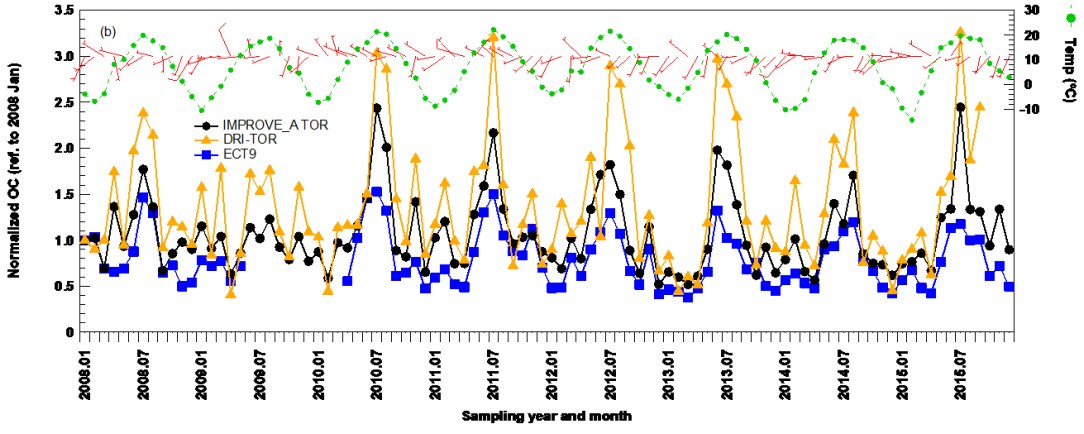

Atmos. Meas. Tech. Discuss., https://doi.org/10.5194/amt-2019-104
Manuscript under review for journal Atmos. Meas. Tech.
Discussion started: 18 April 2019

Atmospheric Measurement Techniques Discussions

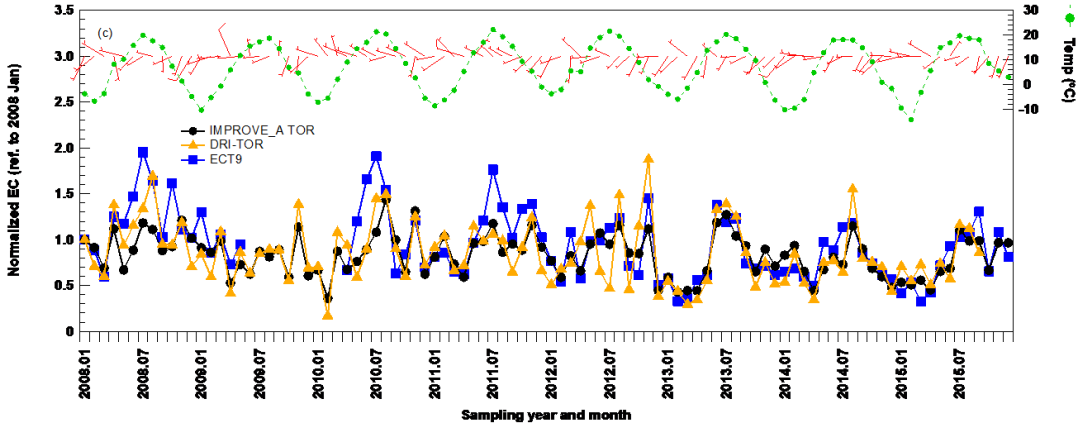

782

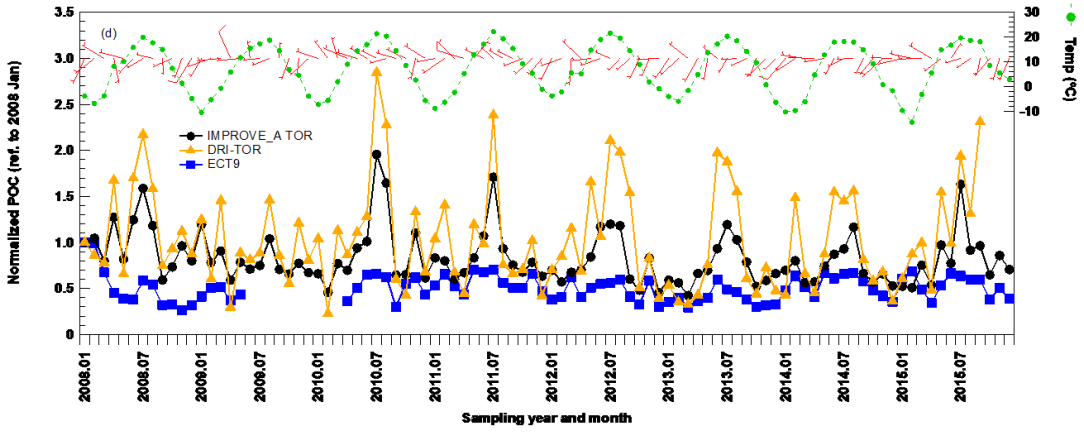

783

784

785

Atmos. Meas. Tech. Discuss., https://doi.org/10.5194/amt-2019-104
Manuscript under review for journal Atmos. Meas. Tech.
Discussion started: 18 April 2019

Atmospheric Measurement Techniques Discussions

786 **Figure 9** Comparison of the normalized (a) TC, (b) OC, (c) EC, and (d) POC for the CAPMoN (in circles) and
787 CABM (in squares) networks against IMPROVE during summer (May-Oct; in yellow) and winter (Nov-Apr;
788 in black) seasons. The black solid line represent the best-fitted regression line through the origin of all
789 measurements.

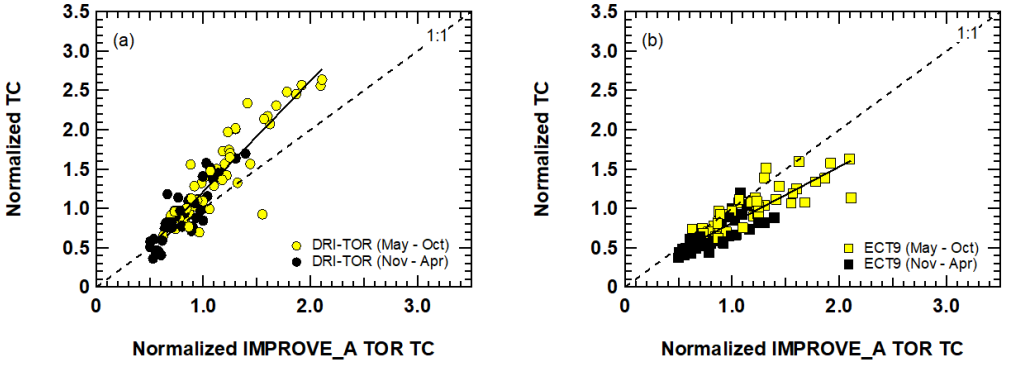

790

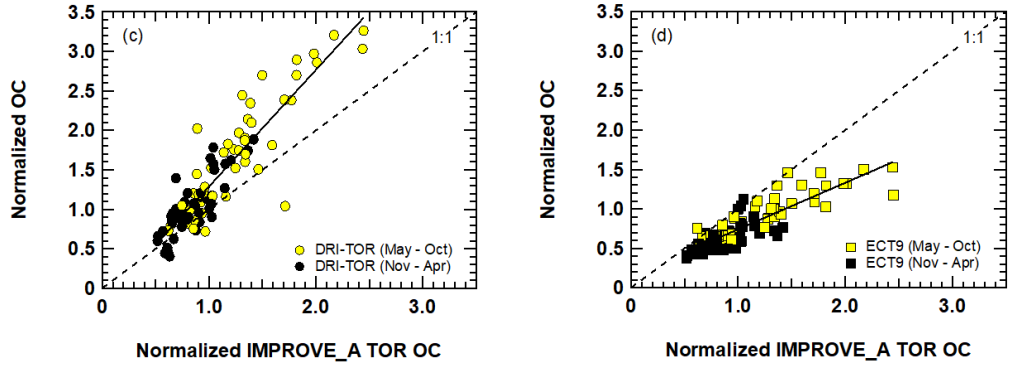

791

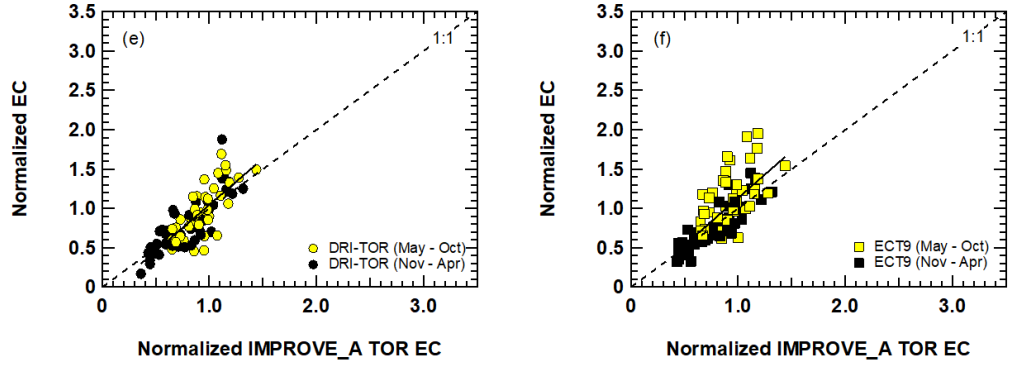

792

Atmos. Meas. Tech. Discuss., https://doi.org/10.5194/amt-2019-104
Manuscript under review for journal Atmos. Meas. Tech.
Discussion started: 18 April 2019

Atmospheric Measurement Techniques Discussions

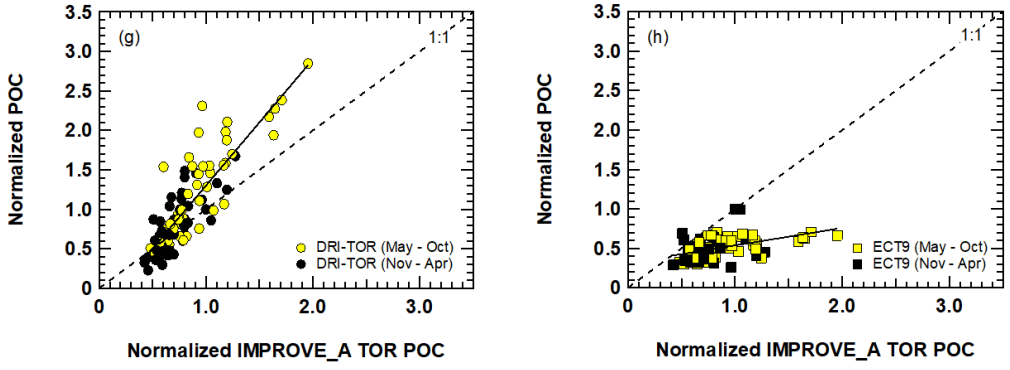

793

794

795 **Figure 10** Figure shows the relationship of averaged (a) TC, (b) OC, and (c) EC concentrations from all
796 networks as a function of ambient temperature. Each data point represent the average value of all
797 network measurements within a 3°C temperature range. Uncertainties are standard deviations of the
798 measurements. Red curve represents the best-fitted Sigmoid function. Figure 10(d) shows the
799 seasonality of ECT9 POC compared to the average OC and EC seasonality. Black solid curve represents
800 the best-fitted Sigmoid function on all ECT9 POC measurements.

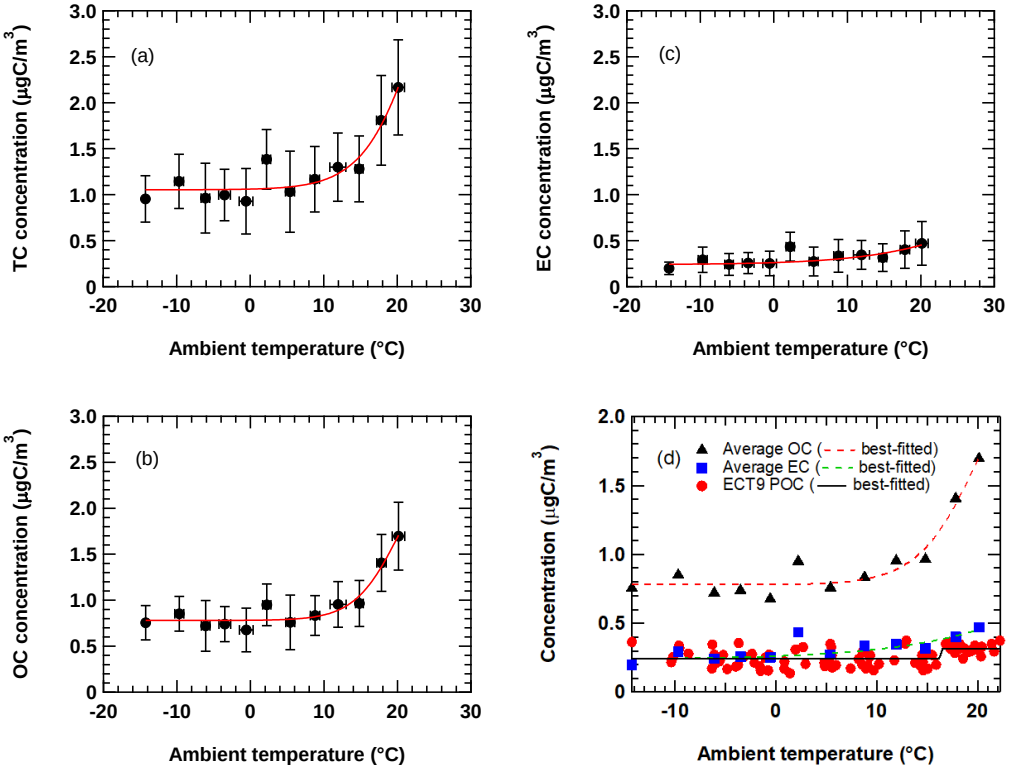

801

802